

AD \_\_\_\_\_

Award Number: DAMD17-01-1-0239

TITLE: Validate Mitotic Checkpoint and Kinetochore Motor Proteins in Breast Cancer Cells as Targets for the Development of Novel Anti-Mitotic Drugs

PRINCIPAL INVESTIGATOR: Timothy J. Yen, Ph.D.

CONTRACTING ORGANIZATION: Fox Chase Cancer Center  
Philadelphia, PA 19111-2497

REPORT DATE: July 2005

TYPE OF REPORT: Final

PREPARED FOR: U.S. Army Medical Research and Materiel Command  
Fort Detrick, Maryland 21702-5012

DISTRIBUTION STATEMENT: Approved for Public Release;  
Distribution Unlimited

The views, opinions and/or findings contained in this report are those of the author(s) and should not be construed as an official Department of the Army position, policy or decision unless so designated by other documentation.

20051107 290

# REPORT DOCUMENTATION PAGE

Form Approved  
OMB No. 0704-0188

Public reporting burden for this collection of information is estimated to average 1 hour per response, including the time for reviewing instructions, searching existing data sources, gathering and maintaining the data needed, and completing and reviewing this collection of information. Send comments regarding this burden estimate or any other aspect of this collection of information, including suggestions for reducing this burden to Department of Defense, Washington Headquarters Services, Directorate for Information Operations and Reports (0704-0188), 1215 Jefferson Davis Highway, Suite 1204, Arlington, VA 22202-4302. Respondents should be aware that notwithstanding any other provision of law, no person shall be subject to any penalty for failing to comply with a collection of information if it does not display a currently valid OMB control number. PLEASE DO NOT RETURN YOUR FORM TO THE ABOVE ADDRESS.

|  |                  |                         |                                      |  |   |
|--|------------------|-------------------------|--------------------------------------|--|---|
| 1. REPORT DATE (DD-MM-YYYY)<br>01-07-2005  |                  | 2. REPORT TYPE<br>Final |                                      | 3. DATES COVERED (From - To)<br>1 Jul 2001 – 30 Jun 2005 |   |
| 4. TITLE AND SUBTITLE<br>Validate Mitotic Checkpoint and Kinetochore Motor Proteins in Breast Cancer Cells as Targets for the Development of Novel Anti-Mitotic Drugs  |                  |                         |                                      | 5a. CONTRACT NUMBER                                      |   |
|  |                  |                         |                                      | 5b. GRANT NUMBER<br>DAMD17-01-1-0239                     |   |
|  |                  |                         |                                      | 5c. PROGRAM ELEMENT NUMBER                               |   |
| 6. AUTHOR(S)<br>Timothy J. Yen, Ph.D.<br><br>E-mail: timothy.yen@fccc.edu  |                  |                         |                                      | 5d. PROJECT NUMBER                                       |   |
|  |                  |                         |                                      | 5e. TASK NUMBER  |   |
|  |                  |                         |                                      | 5f. WORK UNIT NUMBER                                     |   |
| 7. PERFORMING ORGANIZATION NAME(S) AND ADDRESS(ES)<br><br>Fox Chase Cancer Center<br>Philadelphia, PA 19111-2497   |                  |                         |                                      | 8. PERFORMING ORGANIZATION REPORT NUMBER                 |   |
| 9. SPONSORING / MONITORING AGENCY NAME(S) AND ADDRESS(ES)<br>U.S. Army Medical Research and Materiel Command<br>Fort Detrick, Maryland 21702-5012  |                  |                         |                                      | 10. SPONSOR/MONITOR'S ACRONYM(S)                         |   |
|  |                  |                         |                                      | 11. SPONSOR/MONITOR'S REPORT NUMBER(S)                   |   |
| 12. DISTRIBUTION / AVAILABILITY STATEMENT<br>Approved for Public Release; Distribution Unlimited   |                  |                         |                                      |  |   |
| 13. SUPPLEMENTARY NOTES  |                  |                         |                                      |  |   |
| 14. ABSTRACT<br>Drugs that inhibit microtubule functions are one of many anti-neoplastic drugs that are used to combat breast and other cancers. Taxol and vincristine are microtubule poisons that block the proper function of microtubules that are essential for a broad spectrum of motile biological processes that include cell division, vesicle transport, cell shape, and flagella functions. For rapidly proliferating cancer cells, anti-microtubule drugs offers a highly effective means to block cell division and thus stop tumor growth. Nevertheless, these drugs block other microtubule dependent processes that adversely affect the functions of many non-dividing cells. Furthermore, there is the complication that the cancer cells can develop multi-drug resistance that makes them refractile to conventional anti-neoplastic agents. The identification of novel drugs with increased selectivity towards mitotic processes and act synergistically with existing anti-microtubule drugs should enhance and refine the modalities used to treat breast cancer patients. Our interest in the molecular and biochemical mechanisms that are central to mitosis in human cells has led to the identification of novel proteins and pathways that are suited for designing highly specific anti-mitotic drugs. The objective of this proposal is to disrupt such pathways in established breast cancer cell lines to validate them as suitable targets for developing new anti-mitotic drugs. |                  |                         |                                      |  |   |
| 15. SUBJECT TERMS<br>Mitosis, microtubules, kinetochores, spindle checkpoint   |                  |                         |                                      |  |   |
| 16. SECURITY CLASSIFICATION OF:  |                  |                         | 17. LIMITATION OF ABSTRACT<br><br>UU | 18. NUMBER OF PAGES<br><br>43                            | 19a. NAME OF RESPONSIBLE PERSON           |
| a. REPORT<br>U   | b. ABSTRACT<br>U | c. THIS PAGE<br>U       |                                      |  | 19b. TELEPHONE NUMBER (include area code) |

## Table of Contents

|  |    |
|--|----|
| Front Cover .....                        | 1  |
| Standard Form 298 .....                  | 2  |
| Table of Contents .....                  | 3  |
| Introduction .....                       | 4  |
| Body .....                               | 4  |
| Key Research Accomplishments .....       | 9  |
| Reportable Outcomes .....                | 9  |
| (including Bibliography of Publications) |    |
| Conclusions .....                        | 9  |
| References .....                         | NA |
| List of Personnel .....                  | 10 |
| Appendices .....                         | 10 |

### **Introduction:**

Drugs that inhibit microtubule functions are one of many anti-neoplastic drugs that are used to combat breast and other cancers. Taxol and vincristine are microtubule poisons that block the proper function of microtubules that are essential for a broad spectrum of motile biological processes that include cell division, vesicle transport, cell shape, and flagella functions. For rapidly proliferating cancer cells, anti-microtubule drugs offers a highly effective means to block cell division and thus stop tumor growth. Nevertheless, these drugs block other microtubule dependent processes that adversely affect the functions of many non-dividing cells. Furthermore, there is the complication that the cancer cells can develop multi-drug resistance that makes them refractile to conventional anti-neoplastic agents. The identification of novel drugs with increased selectivity towards mitotic processes and act synergistically with existing anti-microtubule drugs should enhance and refine the modalities used to treat breast cancer patients. Our interest in the molecular and biochemical mechanisms that are central to mitosis in human cells has led to the identification of novel proteins and pathways that are suited for designing highly specific anti-mitotic drugs. The objective of this proposal is to disrupt such pathways in established breast cancer cell lines to validate them as suitable targets for developing new anti-mitotic drugs.

### **Body:**

We proposed to manipulate two pathways that are known to be essential and operate only in mitosis of human cells to validate them as suitable targets for the development of novel anti-neoplastic agents. One pathway is specified by the kinesin-like motor protein CENP-E that is essential for aligning chromosomes at the spindle equator during mitosis. The second pathway is a checkpoint pathway that is specified by multiple proteins to ensure cells do not prematurely exit mitosis in the presence of unaligned chromosomes. We proposed four tasks to achieve our goals. We have chosen to analyze three established breast cancer lines and compare their responses to the HeLa cervical carcinoma cell line, with which we have studied these two pathways extensively.

**Task 1.** Evaluate expression of mitotic proteins CENP-E and checkpoint proteins in established breast cancer lines.

We have conducted immunoblot analysis to determine the expression of CENP-E and the checkpoint proteins, hBUB1, hBUBR1, MAD1, MAD2 and Cdc20 in MCF7, T47D, MDA 231 and MDA468 cells. Most of these proteins were found to be expressed in these cell lines and thus confirmed that they are valid *in vivo* targets (Figure 1). The exceptions were that BubR1 expression was low in MCF7 while Mad2 expression was low in T47D cells, when compared with the other cell lines. In addition to these proteins, we also probed for expression of several other kinetochore proteins whose functions are now known to be important for the mitosis. These include CENPI, CENP-F, ZW10 and Nuf2. We have determined that all of these proteins are localized to kinetochores in MCF7 and MDA-468 cells. Figures 2 and 4 show localization of hBUB1 and CENP-E to kinetochores of mitotic MCF7 and MDA468 cells, respectively. The presence of CENP-E and various checkpoint proteins at kinetochores support our prediction that these proteins provide similar functions in mitosis as we have shown in Hela cells.

We have also examined the response of MCF7 and MDA468 cells to the microtubule inhibitor, nocodazole and found that this drug will delay cells in mitosis. These findings indicate that the mitotic checkpoint pathway is likely to be intact in these cancer cell lines. Thus, the various checkpoint proteins that we proposed to analyze in this project are strong candidates with which we can use to inhibit this pathway.

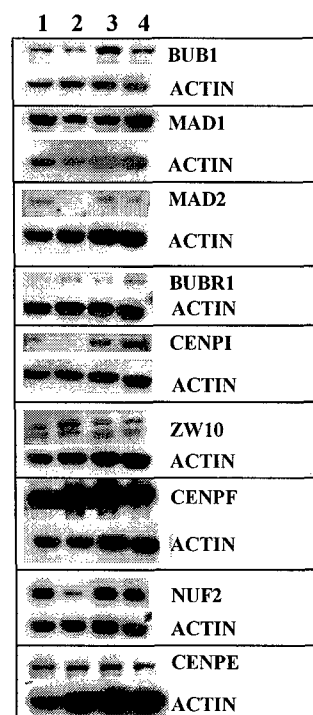


**Fig. 1.** Expression profile of nine kinetochore proteins in breast cancer cell lines. MCF7 (1), T47D (2), MDA-231 (3) and MDA468 (4) were probed with indicated antibodies. Actin was used as a loading control.

**Task 2.** Evaluate response of T47D, MCF-7 and MDA-MB-468 cells to inhibition of the mitotic checkpoint proteins, hBUBR1, hBUB3, cdc20 and MAD2.

As we have confirmed that these breast cancer lines express the target mitotic checkpoint proteins, we have initiated efforts to inhibit the mitotic checkpoint. We had originally proposed to accomplish this by microinjecting antibodies and overexpression of dominant negative mutants. However, new advances in silencing gene expression by RNA interference (RNAi) have altered our original strategy.

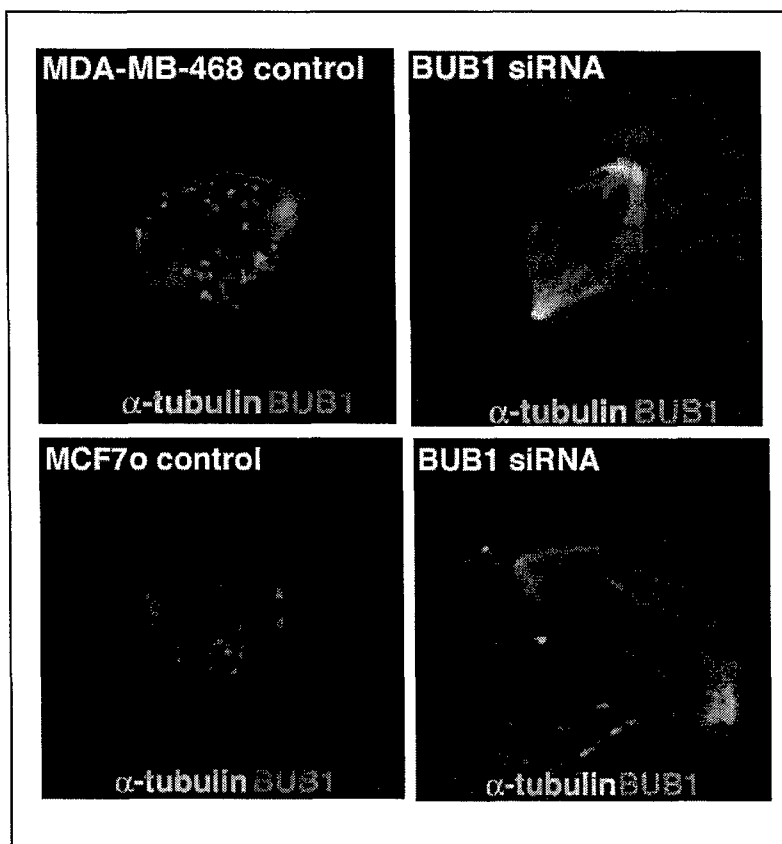
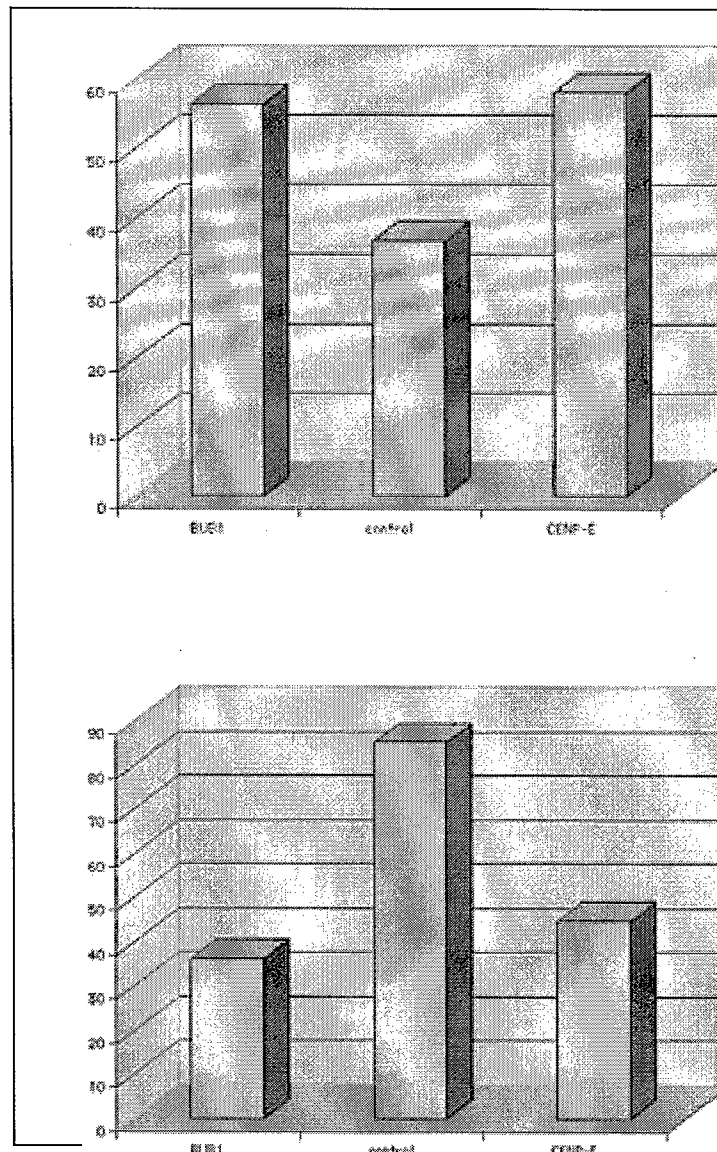


**Figure 2.** MDA468 and MCF cells were trans-fected with a control (left panels) or BUB1 (right panels) siRNAs and mitotic cells were stained with rabbit anti-hBub1, mouse anti-tubulin and DNA. Images were captured with a 63X oil objective and then pseudo-colored and merged.

Using siRNA, we have successfully inhibited the expression of hBUB1 kinase in Hela cells. One unexpected finding was that the loss of hBUB1 prevented the assembly of MAD1, MAD2 and hBUBR1 checkpoint proteins to the kinetochore (data not shown). Thus, inhibition of hBUB1 kinase may result in the inhibition of multiple checkpoint proteins. Based on these studies, we have transfected MCF7 and MDA468 cells with hBUB1 siRNA. At the single cell level, it is clear that hBUB1 expression can be reduced by siRNA (Figure 1). However, the low transfection efficiencies of these cell lines have made it difficult to interpret results from clonogenic experiments. While there are instances where cells transfected with hBUB1 siRNA exhibited reduced efficiency of colony formation (Figure 2), this outcome is highly variable.

We attribute this to the variability in transfection efficiencies of MCF7 and MDA468 cells. To overcome this obstacle, we plan to infect cells with a recombinant lentivirus that express the siRNA of interest. This viral delivery system was developed to overcome problems with poor transfection efficiencies. We are in the process of making the appropriate constructs so that we may generate large stocks of recombinant lentivirus for the clonogenic studies.

**Figure 3.** MCF7 (top panel) and MDA-468 (bottom panel) cells were transfected with BUB1 (left), control (center) and CENP-E (right) siRNAs and were plated at approximately 200 cells per 35cm plate. Colonies were stained and counted on day 15 for MCF7 and day 11 for MDA468. Left axis represents colony number.



**Task 3.** Evaluate CENP-E as a target to block T47D, MCF-7 and MDA-MB-468 cells in mitosis.

As with our studies of the checkpoint pathway, we have opted to inhibit CENP-E function by RNAi technology. Using HeLa cells as a positive control, we succeeded to inhibit expression of CENP-E and cells arrest in mitosis because chromosomes fail to align properly (data not shown). As before, we are able to reduce CENP-E expression in MCF7 and MDA468 cells at the single cell level. We are therefore also generating recombinant lentivirus that express CENP-E RNAi so that we may conduct our clonogenic survival studies.

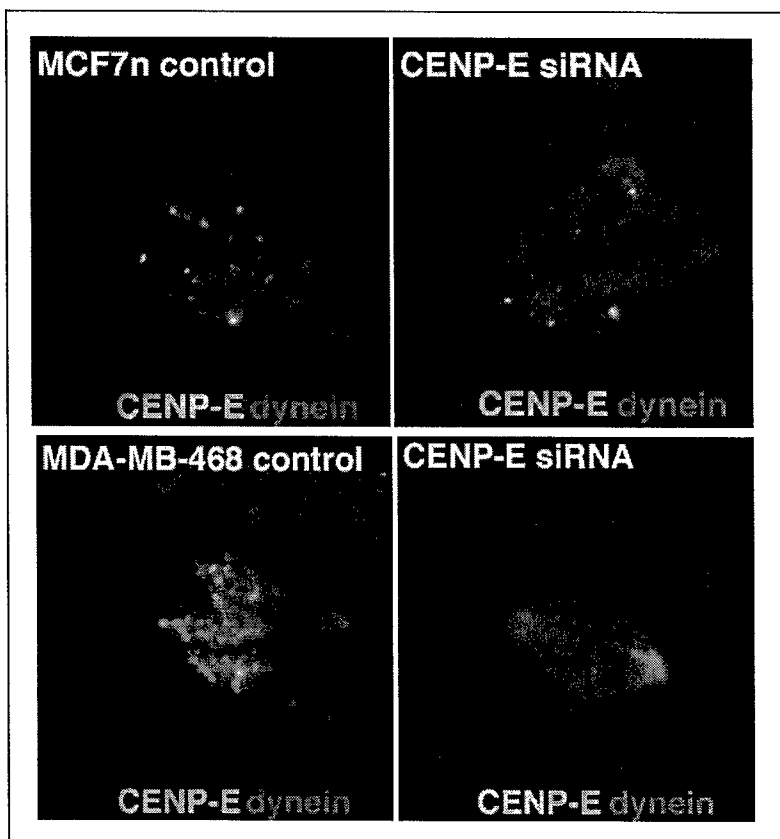


**Figure 4.** MDA468 and MCF cells were trans-fected with a control (left panels) or CENP-E (right panels) siRNAs and mitotic cells were stained with rabbit anti-CENP-E, mouse anti-dynein and DNA. Images were captured with a 63X oil objective and then pseudo-colored and merged.

Although not an official aim of this project, we recently obtained the crystal structure of the monomeric motor domain of CENP-E and the results of these studies are now in press. This work was conducted in collaboration with Dr. Kozielski who is a crystallographer. The purpose of this study is to use the structure to design chemical inhibitors of CENP-E. As we have previously shown that the motor domain of CENP-E is critical for its function *in vivo*, such inhibitors would complement the RNAi approach to knockdown CENP-E function. Inhibitors have been identified but they are not cell permeable. Ongoing efforts are to derivatize the compounds to improve cell uptake.

**Task 4.** Maintaining stocks of affinity purified antibodies.

Over the past year, we have generated monoclonal antibodies to hBUB1, hBUBR1 and MAD1 proteins. The existence of monoclonal antibodies to these and other checkpoint proteins provides us with a continuous source of high quality antibody. While the efforts to generate monoclonal antibodies are significant, we are certain that it will reduce the labor that is required to maintain stocks of polyclonal antibodies. We have recently generated a monoclonal antibody against CENP-E. We succeed to generate a Mad2 monoclonal antibody that can be used for immunoprecipitations and western blots but is ineffective for immunocytochemistry. Both monoclonal antibodies have been licensed commercially.



### Key Research Accomplishments:

- Confirmed expression and localization of CENP-E and the mitotic checkpoint proteins hBUB1, hBUBR1, MAD1, MAD2, Cdc20 and CENP-E, in MCF7, T47D, MDA231 and MDA468 cells.
- Optimized and tested a variety of transfection reagents and found a newly developed product that efficiently delivers siRNA into all four cell lines. Prior to this, we had verified using available reagents that siRNA can inhibit the expression of CENP-E and hBUB1 in MCF7 and MDA468 cells.
- Generated monoclonal antibodies to hBUB1, hBUBR1, MAD1, MAD2 and CENP-E.
- Obtained the crystal structure of the CENP-E motor domain.

### Reportable Outcomes including Bibliography of Publications:

Jablonski, S.A., Liu, S.T., Yen, T.J. Targeting the kinetochore for mitosis-specific inhibitors. *Cancer Biol. Ther.* **2**:21-26, 2003. Appended in Annual Report submitted July 2005.

Liu, S.T., van Deursen, J., Yen, T.J. The role of the mitotic checkpoint in maintaining genomic stability. Edited by G. Schatten. *Curr. Top Dev. Biol.* **58**:27-51, 2003. Appended in Annual Report submitted July 2004.

Joseph J, Liu ST, Jablonski SA, **Yen TJ**, Dasso M. The RanGAP1-RanBP2 complex is essential for microtubule-kinetochore interactions in vivo. *Curr Biol.* 2004 **14**:611-7. 2004. Appended in Annual Report submitted July 2004.

García-Saez, I., Yen, T.J., Wade, R.H., Kozielski, F. Crystal structure of the motor domain of the human kinetochore protein CENP-E. *J. Mol. Biol.* **340**:1107-1116. 2004.

Kao G., and **Yen, T.J.** Mitotic checkpoints, aneuploidy and cancer. In: *Genome Instability and Cancer Progression*. Ed. E. Nigg. In press.

Chan, G.K.T., Liu, S.T., **Yen, T.J.** Structure and function of the human kinetochore. *Trends in Cell Biol.* In press, galley proofs not yet available.

Licensed hBUB1, hBUBR1, CENP-E, MAD1 and MAD2 monoclonal antibodies to BD Sciences. Immquest, Novus Biologicals, Chemicon, AbCAM, Sigma.

### Conclusions:

We validated the expression of candidate target genes in various breast cancer lines and have used siRNA to inhibit their expression in these cells. However, the low transfection efficiencies has prevented us from conducting clonogenic survival experiments. Nevertheless, we are optimistic that the viral delivery system will allow populations of cells to be uniformly infected with recombinant lentivirus that express siRNA. This will allow us to reliably evaluate results from clonogenic studies.

The availability of the crystal structure of the motor domain of CENP-E will afford the opportunity to obtain chemical inhibitors that can be used to test for clonogenic assays. This in combination with siRNA will enhance our ability to target multiple mitotic proteins to assess their importance to the viability of breast cancer cells.

**List of Personnel:**

Tim J. Yen, Principal Investigator  
Beatrice Conner, Scientific Technician  
Sandra Jablonski, Research Associate

**Appendices:**

Garcia-Saez, I., Yen, T.J., Wade, R.H., Kozielski, F. Crystal structure of the motor domain of the human kinetochore protein CENP-E. *J. Mol. Biol.* **340**:1107-1116. 2004.

Kao G., and **Yen, T.J.** Mitotic checkpoints, aneuploidy and cancer. In: *Genome Instability and Cancer Progression*. Ed. E. Nigg. In press.



Available online at www.sciencedirect.com



# Crystal Structure of the Motor Domain of the Human Kinetochore Protein CENP-E

Isabel Garcia-Saez<sup>1</sup>, Tim Yen<sup>2</sup>, Richard H. Wade<sup>1</sup> and Frank Kozielski<sup>1\*</sup>

<sup>1</sup>Laboratoire de Microscopie  
Electronique Structurale  
Institut de Biologie Structurale  
(CEA-CNRS-UJF), 41, rue  
Jules Horowitz, 38027 Grenoble  
Cedex 01, France

<sup>2</sup>Institute for Cancer Research  
Fox Chase Cancer Center, 333  
Cottman Avenue, Philadelphia  
PA 19111, USA

The human kinetochore is a highly complex macromolecular structure that connects chromosomes to spindle microtubules (MTs) in order to facilitate accurate chromosome segregation. Centromere-associated protein E (CENP-E), a member of the kinesin superfamily, is an essential component of the kinetochore, since it is required to stabilize the attachment of chromosomes to spindle MTs, to develop tension across aligned chromosomes, to stabilize spindle poles and to satisfy the mitotic checkpoint. Here we report the 2.5 Å resolution crystal structure of the motor domain and linker region of human CENP-E with MgADP bound in the active site. This structure displays subtle but important differences compared to the structures of human Eg5 and conventional kinesin. Our structure reveals that the CENP-E linker region is in a “docked” position identical to that in the human plus-end directed conventional kinesin. CENP-E has many advantages as a potential anti-mitotic drug target and this crystal structure of human CENP-E will provide a starting point for high throughput virtual screening of potential inhibitors.

© 2004 Elsevier Ltd. All rights reserved.

\*Corresponding author

Keywords: CENP-E; crystal structure; kinesin; kinetochore; mitosis

## Introduction

During cell division, chromosomes capture spindle microtubules and congress to the spindle equator. They then separate by moving towards the spindle poles to provide each daughter cell with the same set of genetic information. A highly regulated macromolecular complex, called the kinetochore, connects chromosomes to spindle microtubules. Significant progress has been made in recent years to identify kinetochore-associated proteins and to elucidate their roles during mitosis (reviews<sup>1–5</sup>). Among many other proteins, kinetochore-associated motor proteins such as dynein<sup>6,7</sup> and members of the kinesin family, centromere-associated protein E (CENP-E)<sup>8,9</sup> and mitotic centromere-associated kinesin (MCAK)<sup>10</sup> have been shown to be involved in essential mitotic events.

CENP-E was first discovered in human cells by a monoclonal antibody raised against chromosome

proteins that were enriched for known centromere/kinetochore components.<sup>8</sup> Subsequently, CENP-E was found to be a novel member of the kinesin superfamily.<sup>9</sup> Since the initial discovery, CENP-E has been identified in *Xenopus laevis*,<sup>11</sup> *Drosophila melanogaster*<sup>12</sup> and phylogenetic sequence analysis has identified putative homologues in *Mus musculus*<sup>13</sup> and in *Arabidopsis thaliana*.<sup>14</sup>

The expression of CENP-E in human cells is cell-cycle-dependent. It is low in early G1 phase but increases as cells progress through the cell cycle and peak levels are detected during late G2 phase and mitosis.<sup>8,9,15</sup> Despite its presence throughout the cell cycle, CENP-E is not detected at kinetochores until early prometaphase and remains there until anaphase A, albeit at significantly reduced levels. By anaphase B, CENP-E is also localized to the interzonal microtubules of the mitotic spindle. In telophase cells, CENP-E is concentrated at the midbody until it is eventually degraded quantitatively at the end of mitosis through a cytokinesis-independent mechanism.<sup>16</sup>

Disruption of CENP-E functions by antibody microinjection, transfection of dominant negative mutants, anti-sense or RNAi and gene knockouts has shown that it is essential for some aspects of kinetochore microtubule attachments.<sup>8,17–20</sup>

Abbreviations used: CENP-E, centromere-associated protein E; MT, microtubule; MCAK, mitotic centromere-associated kinesin; MAP, mitogen activated protein; EM, electron microscopy.

E-mail address of the corresponding author:  
frank.kozielski@ibs.fr

CENP-E appears to be essential for monopolar chromosomes to establish bipolar attachments. As the unattached kinetochore of a monopolar chromosome does not encounter microtubules that emanate from the opposite pole at high frequencies, CENP-E is thought to enhance the efficiency by which kinetochores establish stable microtubule attachments. In contrast to monopolar chromosomes, chromosomes that are situated in the center of the spindle are able to establish bipolar attachments as the higher frequencies of microtubule encounters are thought to compensate for the loss of CENP-E. Quantitative electron microscopy (EM) studies revealed that bipolar kinetochores lacking CENP-E are capable of establishing near normal numbers of microtubule attachments.<sup>21</sup> These bipolar connections are nevertheless defective as they are unable to generate sufficient pole-ward force to achieve normal levels of tension between the sister kinetochores.<sup>18,21</sup>

Kinesins belonging to the CENP-E subfamily are significantly bigger than all other members of the superfamily. Human CENP-E is composed of 2663 residues and has three distinct domains: an N-terminal motor domain (residues Met1–Lys327) that includes MT and ATP binding sites, a long discontinuous  $\alpha$ -helix (residues Asn336–Ala2471) and a C-terminal ATP-independent MT-binding domain<sup>22</sup> (residues Gln2472–Gln2663). The kinetochore-binding region is located in the C-terminal part of the protein<sup>23</sup> (residues Ile2126–Val2476). Human CENP-E contains two regions with homology to PEST sequences (residues Arg459–Lys489 and His2480–Lys2488), which might be responsible for rapid intracellular degradation of CENP-E at the end of mitosis.<sup>15</sup> The carboxy-terminal ATP-independent MT binding site (residues Glu2565–Gln2663) in human CENP-E is thought to be regulated *in vivo* by mitotic phosphorylations that inhibit its microtubule binding activity. The presence of several consensus phosphorylation sites for a cyclin B cdc2 kinase complex is consistent with the ability of this kinase to phosphorylate and inhibit microtubule binding in this domain *in vitro*.<sup>22</sup> In addition, the *in vivo* association of CENP-E with mitogen activated protein (MAP) kinase during mitosis suggests there may be an additional regulation mechanism for the interaction between microtubules and chromosomes and thus mitotic progression.<sup>24</sup>

Previous work has established that the critical determinant that specifies the directionality of kinesins along microtubules is a short region, that we refer to as the linker (sometimes called neck), linking the kinesin motor domain to the  $\alpha$ -helical coiled region (short reviews<sup>25,26</sup>). This linker region is found to be distinctly different between plus-ended kinesins whose motor domains are located near the N-terminal end of the polypeptide chain and minus-ended kinesins whose motor domains are located near the C terminus. In the case of CENP-E the current situation is somewhat confusing, since there have been reports of slow plus-

end directed movement,<sup>11</sup> of slow minus-end directed motor activity<sup>27</sup> or simply of microtubule tethering without movement.<sup>28</sup> These discrepancies, along with the considerable importance of human CENP-E, have encouraged us to engage structural studies, and we describe here the first crystal structure of the motor domain of this kinetochore-associated protein.

## Results

A construct with the amino-terminal 342 residues of CENP-E containing the ATP sensitive microtubule binding site along with the ~12 residue linker region was expressed in *Escherichia coli*. N-terminal sequencing of the first seven residues revealed that the first methionine is missing (peptide sequence: AEEGAV) due to bacterial processing.<sup>29</sup> The measured molecular mass of 39,149 Da using electrospray mass spectrometry is in excellent agreement with the predicted mass of 39,152 Da. Gel filtration data (not shown) suggest that CENP-E is monomeric.

The crystal form investigated has two CENP-E molecules (A and B) per asymmetric unit. We ask whether these are indeed two independent monomers. The relative orientations of the two motor domains in the crystal structures of established kinesin dimers, i.e. *Rattus norvegicus* conventional kinesin<sup>30</sup> and *D. melanogaster* ncd,<sup>31</sup> are notably different from those in the asymmetric unit of our CENP-E crystals (data not shown). Since our construct does not extend into the accepted dimerization domain, this suggests that in the present case there are two independent monomers whose relative orientations are due to crystal packing and electrostatic interactions. The residues involved are listed in Table 1. In monomer A, they localize to the end region of  $\beta$ 1c, to  $\alpha$ 4 and to the C-terminal loop between  $\alpha$ 6 and the linker region. In monomer B, they are near the N terminus, mainly in  $\beta$ 1a,  $\beta$ 1b and  $\beta$ 1c (Table 1).

The resolved structure of monomer A includes residues Glu4–Lys216, Gly224–Ala243, Arg251–Ser339, bound MgADP and a molecule of Pipes (1,4-piperazinediethanesulfonic acid) that was present in the crystallization buffer. The final model in monomer B comprises residues Gly5–Asn17, Ala27–Lys216, Ser225–Ala243 and Leu252–Ser339 and bound MgADP. When 304 C $\alpha$  positions in the two monomers were superposed by a least-squares fit, their final r.m.s. deviation after three cycles was 0.72 Å. Only monomer A results are presented here, since its electron density map is clearly better than that of monomer B (Figure 1). This could possibly be due to the presence of more crystal contacts between A and neighboring molecules than for B (results not shown). The final refined model contains 84 water molecules.

Figure 1(A) and (B), shows front and back views of the CENP-E motor domain structure. It has a

**Table 1.** Interactions between monomers A and B in the asymmetric unit of the CENP-E crystal (distances  $\leq 3.5$  Å)

| B               | A    |      |      |      |      |      |      |                   |                   |                   |                   |      |      |      |
|-----------------|------|------|------|------|------|------|------|-------------------|-------------------|-------------------|-------------------|------|------|------|
|                 | N48  | K270 | S273 |      | D274 |      | K327 | Y328              |                   |                   |                   |      |      | K330 |
|                 | ND2  | NZ   | OG   | O    | OD1  | OD2  | NZ   | CG                | CD1               | CD2               | CE1               | CE2  | OH   | NZ   |
| D42             |      |      |      |      |      |      |      |                   |                   |                   |                   |      |      |      |
| OD1             | 2.51 |      |      |      |      |      |      |                   |                   |                   |                   |      |      |      |
| D42             |      |      |      |      |      |      |      |                   |                   |                   |                   |      |      |      |
| OD2             | 3.36 |      |      |      |      |      |      |                   |                   |                   |                   |      |      |      |
| D34             |      |      |      |      |      |      |      |                   |                   |                   |                   |      |      |      |
| OD2             |      | 2.74 |      |      |      |      |      |                   |                   |                   |                   |      |      |      |
| Y39             |      |      |      |      |      |      |      |                   |                   |                   |                   |      |      |      |
| OH <sup>a</sup> |      |      | 3.17 | 3.40 |      | 2.38 |      |                   |                   |                   |                   |      |      |      |
| N35             |      |      |      |      |      |      |      |                   |                   |                   |                   |      |      |      |
| ND2             |      |      |      |      | 2.85 |      |      |                   |                   |                   |                   |      |      |      |
| G43             |      |      |      |      |      |      |      |                   |                   |                   |                   |      |      |      |
| O               |      |      |      |      |      |      | 3.20 |                   |                   |                   |                   |      |      |      |
| Y39             |      |      |      |      |      |      |      |                   |                   |                   |                   |      |      |      |
| CD2             |      |      |      |      |      |      |      | 3.29 <sup>b</sup> | 3.27 <sup>b</sup> | 3.48 <sup>b</sup> | 3.48 <sup>b</sup> |      |      |      |
| K45             |      |      |      |      |      |      |      |                   |                   |                   |                   |      |      |      |
| O               |      |      |      |      |      |      |      |                   |                   | 3.31              |                   | 3.21 |      |      |
| Q40             |      |      |      |      |      |      |      |                   |                   |                   |                   |      |      |      |
| O               |      |      |      |      |      |      |      |                   |                   |                   |                   |      | 2.92 |      |
| S44             |      |      |      |      |      |      |      |                   |                   |                   |                   |      |      |      |
| O               |      |      |      |      |      |      |      |                   |                   |                   |                   |      |      | 3.37 |

<sup>a</sup> One of the two conformations of Y39B.<sup>b</sup> Hydrophobic interactions between the side-chains of Tyr328 and Tyr39.

mixed eight-stranded  $\beta$ -sheet core with flanking solvent-exposed  $\alpha$ -helices and a small three-stranded antiparallel  $\beta$ -sheet in the N-terminal region. Interestingly, the linker region (Figure 1(B)) (residues Tyr328–Ser339), has the same docked conformation as found in *R. norvegicus* KHC<sup>30,32</sup> and in one of the *Homo sapiens* KHC structures.<sup>33</sup> Linker region, residues in  $\beta 9$  and  $\beta 10$ , form main-chain hydrogen bonds with  $\beta 8$  and  $\beta 7$ , respectively, in the motor domain core giving short antiparallel  $\beta$ -sheets between  $\beta 8$ – $\beta 9$  and  $\beta 7$ – $\beta 10$ . The following amino acid residues are involved: Asn336 N and the O atom of Gly77, O of Asn336 with Val228 N, Val338 N with V226 O, and V338 O with V226 N. There are also electrostatic interactions between the side-chains of Asn336 and Asn79. A water molecule, Wat59, plays a structural role in the stabilization of the “cross-road” between the residues of the motor domain and the linker by forming hydrogen bonds with Asn79 N (located in the N-terminal part of  $\beta 3$ ), Asn299 ND2 (located in loop 13 after  $\alpha 5$ ) and the linker Tyr334 O and Asn336 OD1.

MgADP and three water molecules are located in the nucleotide-binding pocket (Figures 1 and 2). The Mg ion interacts with two  $\beta$ -phosphate oxygen moieties, with three water molecules and with the hydroxyl moiety of Thr93 at the end of the P-loop motif. The interactions between MgADP and specific amino acid residues in the pocket are listed in Table 2. The expected position for  $\gamma$ -phosphate is empty. Curiously, a molecule of Pipes, from the buffer, is located in a pocket some 15.3 Å away (data not shown). The bottom of this pocket is formed by the beginning of helix  $\alpha 5$ , and the

“walls” by a turn between  $\beta 4$  and  $\beta 5$  and the N-terminal part of helix  $\alpha 4$ . A residue that has a double conformation, Ser261, contacts the Pipes molecule.

## Discussion

CENP-E is a very important component of the kinetochore during mitosis where it is essential both for the stable bi-oriented attachment of chromosomes to spindle microtubules and for chromosome movements leading to congression. Currently, however, the reported interactions with microtubules are largely ambiguous and raise the following question. Can this kinesin support directed movement along microtubules and is this compatible with reported chromosome transport towards the minus ends of depolymerising microtubules?<sup>34</sup>

To determine whether there is some unique structural explanation that may explain the different accounts of CENP-E motor activity, we have solved the crystal structure of the CENP-E motor domain. The linker region, with the two short  $\beta$  strands,  $\beta 9$  and  $\beta 10$  (Tyr228–Ser339) is particularly interesting. This region has the same docked conformation found for other N-terminal motor domain kinesins, human KHC and Eg5<sup>35</sup> and rat KHC. From the structural point of view, therefore, CENP-E appears to have all the features of a plus-end directed kinesin: the motor domain is in the N-terminal region of the polypeptide chain and it has a linker region conforming to the N-type kinesin model. This is consistent with the

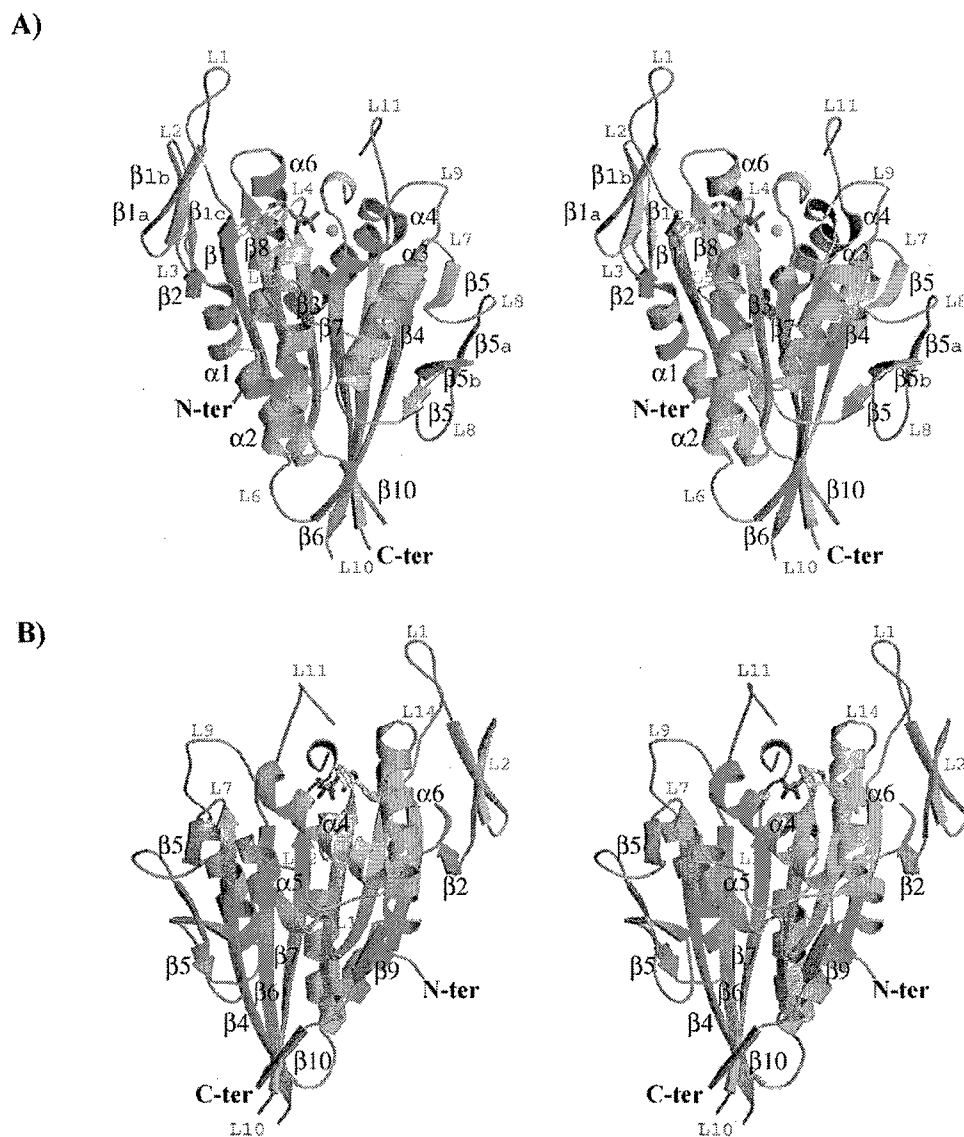


**Figure 1.** Stereo plot of the CENP-E motor domain structure.  $\beta$ -Strands are colored in green,  $\alpha$ -helices in blue and loops in yellow. The linker region (containing  $\beta 9$  and  $\beta 10$ ) is colored in red. Bound MgADP in the nucleotide-binding pocket is displayed as a ball and stick model. The numbering of the secondary structure elements is that used by Kull and co-workers.<sup>54</sup> (A) Front view. (B) Back view, rotated 180° with respect to (A).

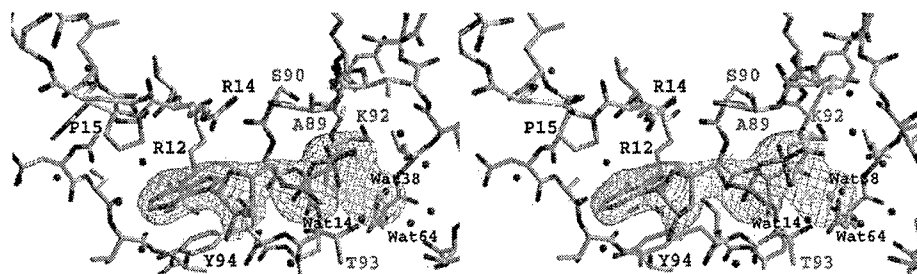


**Figure 2.** Structure of the nucleotide-binding site of human CENP-E. The electron density for MgADP is depicted. P-loop residues are indicated in red. Three conserved water molecules in contact with MgADP are labeled.

**Table 2.** Main ADP interactions with the nucleotide binding site of CENP-E (distances <3.5 Å)

| CENP-E | ADP atoms |      |      |      |      |      |      |                 |                 |                   |      |      |
|--------|-----------|------|------|------|------|------|------|-----------------|-----------------|-------------------|------|------|
|        | PB        | O1B  | O2B  | O3B  | O1A  | O2A  | O3A  | C4 <sup>a</sup> | O4 <sup>a</sup> | C6                | N6   | N1   |
| A89    |           |      |      |      |      |      |      |                 |                 |                   |      |      |
| N      | 3.34      |      |      | 2.79 |      |      | 3.38 |                 |                 |                   |      |      |
| S90    |           |      |      |      |      |      |      |                 |                 |                   |      |      |
| N      |           | 3.47 |      |      |      |      |      |                 |                 |                   |      |      |
| G91    |           |      |      |      |      |      |      |                 |                 |                   |      |      |
| N      |           | 3.32 |      |      |      |      | 3.46 |                 |                 |                   |      |      |
| K92    |           |      |      |      |      |      |      |                 |                 |                   |      |      |
| N      |           | 2.91 |      |      |      |      |      |                 |                 |                   |      |      |
| K92    |           |      |      |      |      |      |      |                 |                 |                   |      |      |
| NZ     |           | 3.00 |      |      |      |      |      |                 |                 |                   |      |      |
| T93    |           |      |      |      |      |      |      |                 |                 |                   |      |      |
| N      |           |      | 2.97 |      | 3.41 |      |      |                 |                 |                   |      |      |
| T93    |           |      |      |      |      |      |      |                 |                 |                   |      |      |
| OG1    |           |      | 3.16 |      |      |      |      |                 |                 |                   |      |      |
| Y94    |           |      |      |      |      |      |      |                 |                 |                   |      |      |
| N      |           |      |      |      | 2.93 |      |      |                 |                 |                   |      |      |
| R14    |           |      |      |      |      |      |      |                 |                 |                   |      |      |
| NH2    |           |      |      |      |      |      |      | 3.41            | 2.99            |                   |      |      |
| P15    |           |      |      |      |      |      |      |                 |                 |                   |      |      |
| CD     |           |      |      |      |      |      |      |                 |                 | 3.41 <sup>a</sup> |      |      |
| R12    |           |      |      |      |      |      |      |                 |                 |                   |      |      |
| NH2    |           |      |      |      |      |      |      |                 |                 |                   | 3.35 |      |
| Mg     | 3.49      |      | 2.36 | 3.40 |      |      |      |                 |                 |                   |      |      |
| Wat14  |           |      | 3.06 |      |      | 2.60 |      |                 |                 |                   |      |      |
| Wat53  |           |      |      |      |      |      |      |                 |                 |                   |      | 3.33 |

<sup>a</sup> Hydrophobic interactions.

plus-end activity exhibited by *Xenopus* CENP-E. Nevertheless, the directionality of human CENP-E remains to be verified by *in vitro* motility assays using expressed dimer constructs.

Another interesting feature is that linker docking has been reported to be due to the presence of sulfate ions, mimicking inorganic phosphate, in specific cavities close to the nucleotide binding site.<sup>33</sup> In the present case no sulfate was present in the crystallization buffer and no density is visible in the same cavities. Consequently, the hypothetical role of the "phosphate cavities" for linker docking appears to be in question.

A large number of kinesins are now known and this superfamily has ten or more phylogenetic subgroups as established by detailed comparisons of their motor domain amino acid sequences.<sup>14</sup> Each subgroup appears to be associated with a specific function at different stages of the cell cycle. Apart from the criterion of overall sequence similarity, each subfamily is also clearly characterized by specifically located sequence insertions and deletions.<sup>36</sup> Thus, it appears that subfamily specific functionality may be related to subtle structural differences introduced by these insertions and deletions. The two other motor domain structures of kinesin superfamily members in *H. sapiens* that have been determined are conventional kinesin,<sup>33</sup> involved in intracellular transport, and Eg5<sup>35</sup> responsible for stabilization of the bipolar spindle in mitosis.<sup>37</sup> Since human CENP-E, Eg5 and KHC belong to distinct phylogenetic subgroups, we have compared their structures so as to visualize subfamily specific structural features (Figures 3 and 4).

The sequence identity between the motor domains of CENP-E and KHC is 38.0% and the r.m.s. deviation between their crystal structures is 1.1 Å after least-squares alignment of 284 C<sup>α</sup> atoms. The identity between CENP-E–Eg5 is 36.1% and the r.m.s. deviation is 1.5 Å for least-squares alignment of 256 C<sup>α</sup> atoms. Compared to KHC, CENP-E has the following subfamily specific insertions and deletions: a two residue insert in loop 2, a three residue deletion in loop 5, a five residue insert in loop 10, a two residue insert in loop 12, and a two residue deletion at the beginning of α6 (Figure 5). Particularly striking is the loop 2 between β1b and β1c, slightly longer than in KHC. This loop is oriented perpendicular to the equivalent loop in Eg5 that has a long insertion. Helix α2 is interrupted by loop 5 in all kinesin motor domain structures so far resolved. This loop is only seven residues long in CENP-E, which is shorter than for any other N-terminal motor domain kinesin. Interestingly, in Eg5 this loop has a seven residue insert compared to KHC and this insert is characteristic of the subfamily (this subfamily is also known as BimC or N2). It is not known whether this region has any specific function as it is on the opposite face to the commonly accepted microtubule interaction region. One disordered region in CENP-E is the "tip" of the arrow-shaped structure, the loop 10 between β6 and β7. This region, from Lys216 to Ser225, is not visible in our electron density map. In CENP-E this loop has five additional residues compared to KHC and it is probably highly flexible, since it is visible in both the KHC and Eg5 structures. Finally, at the C-terminal end of the motor domain core

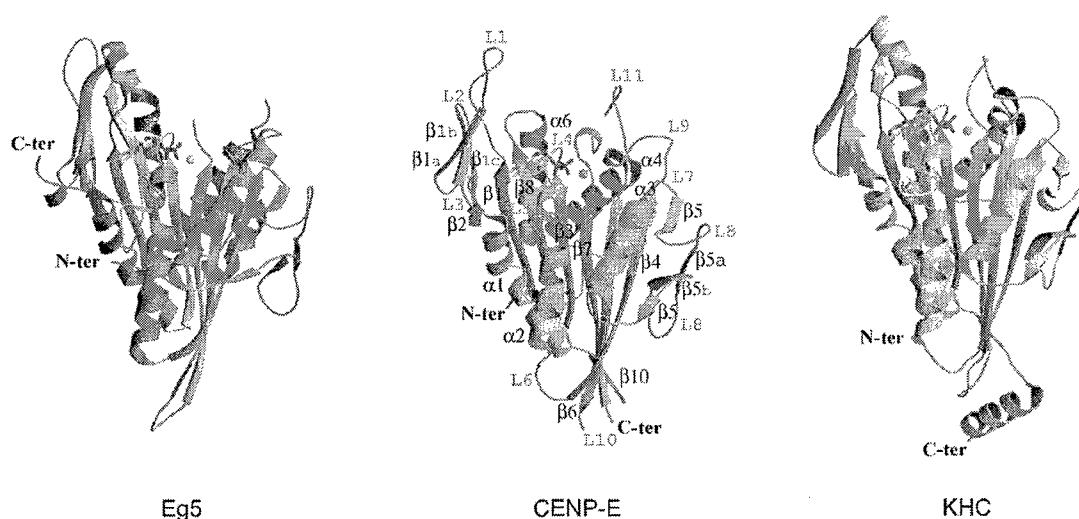


Figure 3. Comparison of the motor domain crystal structures of three human kinesins, Eg5, CENP-E and KHC.

structure, the helix  $\alpha 6$  is two residues shorter in human CENP-E, and in other members of the sub-family, than in any other kinesin.

The active site structures of human KHC, Eg5 and CENP-E are highly conserved. The three water molecules in the CENP-E nucleotide-binding pocket that coordinate with ADP and the Mg ion are also found in the Eg5 and KHC structures (Figure 3). Nevertheless, conserved Arg14 and Pro15 of the N-4 motif (residues Arg12–Pro15), described to be involved in the binding of the purine moiety, are in different positions in CENP-E, since loop 1 immediately after  $\beta 1$  (from Leu16) shows high flexibility and is positioned differently compared to KHC and Eg5 which both contain two turn  $\alpha$ -helices in this region (Figure 4). Particularly, the Arg14 side-chain interacts with the oxygen atom in the ribose ring (Figure 4).

The phosphate-binding loop (P-loop, or motif N-1) (residues Gly86–Thr93), involved in the interaction with  $\alpha$  and  $\beta$ -phosphate groups of the

nucleotide, is structurally conserved in CENP-E, Eg5 and KHC (Figure 4). Concerning the nucleotide state sensing areas, the switch 1 (N-2, residues Asn197–His204), binding motif for the  $\gamma$ -phosphate, appears to be in slightly different positions in Eg5 and KHC (Figure 4), mainly Asn197 and Gln198, compared to CENP-E where the region immediately before these residues (loop 9) is disordered. Nevertheless, switch 1 is similar in the three structures. Switch 2 (N-3 motif) is also involved in binding the  $\gamma$ -phosphate group. It is located immediately after  $\beta 7$  (residues Asp235–Glu240) and differences in this region in CENP-E occur at the beginning of loop 11. Helix  $\alpha 4$  in the switch 2 cluster is in an up conformation that is correlated with the docking of the CENP-E linker as in human and rat KHC.<sup>33,30</sup>

As previously described for the human mitotic kinesin Eg5,<sup>38–40</sup> the discovery of specific inhibitors of the kinetochore-associated CENP-E has considerable interest for future anti-mitotic therapies. The advantages of human CENP-E as a potential drug target have been recently reviewed.<sup>41,42</sup> These include its apparently complete degradation at the end of the mitotic event,<sup>9</sup> and the absence of any additional role of CENP-E in interphase. The crystal structure of human CENP-E will therefore provide a starting point for high-throughput virtual screening of potential inhibitors and as the basis for the structure determination of future CENP-E inhibitor complexes.

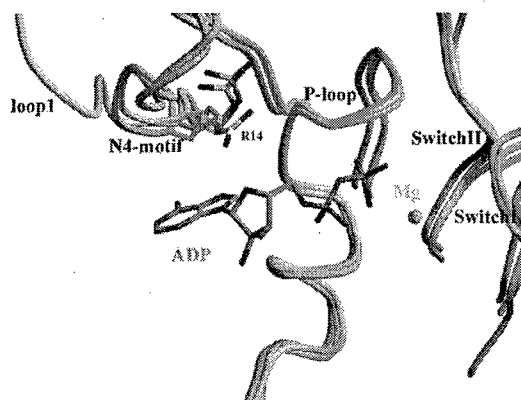


Figure 4. Superposition of the P-loop area of human KHC (yellow), Eg5 (green) and CENP-E (grey). The MgADP is taken from the CENP-E structure.

## Materials and Methods

### Construction of plasmids for protein expression

The DNA construct coding for the human CENP-E motor domain was synthesized by PCR, using the following forward and reverse primers: CENP-E\_1, 5'-CCA GTT CAG CCT GAT ACC ATG GCG GAG GAA



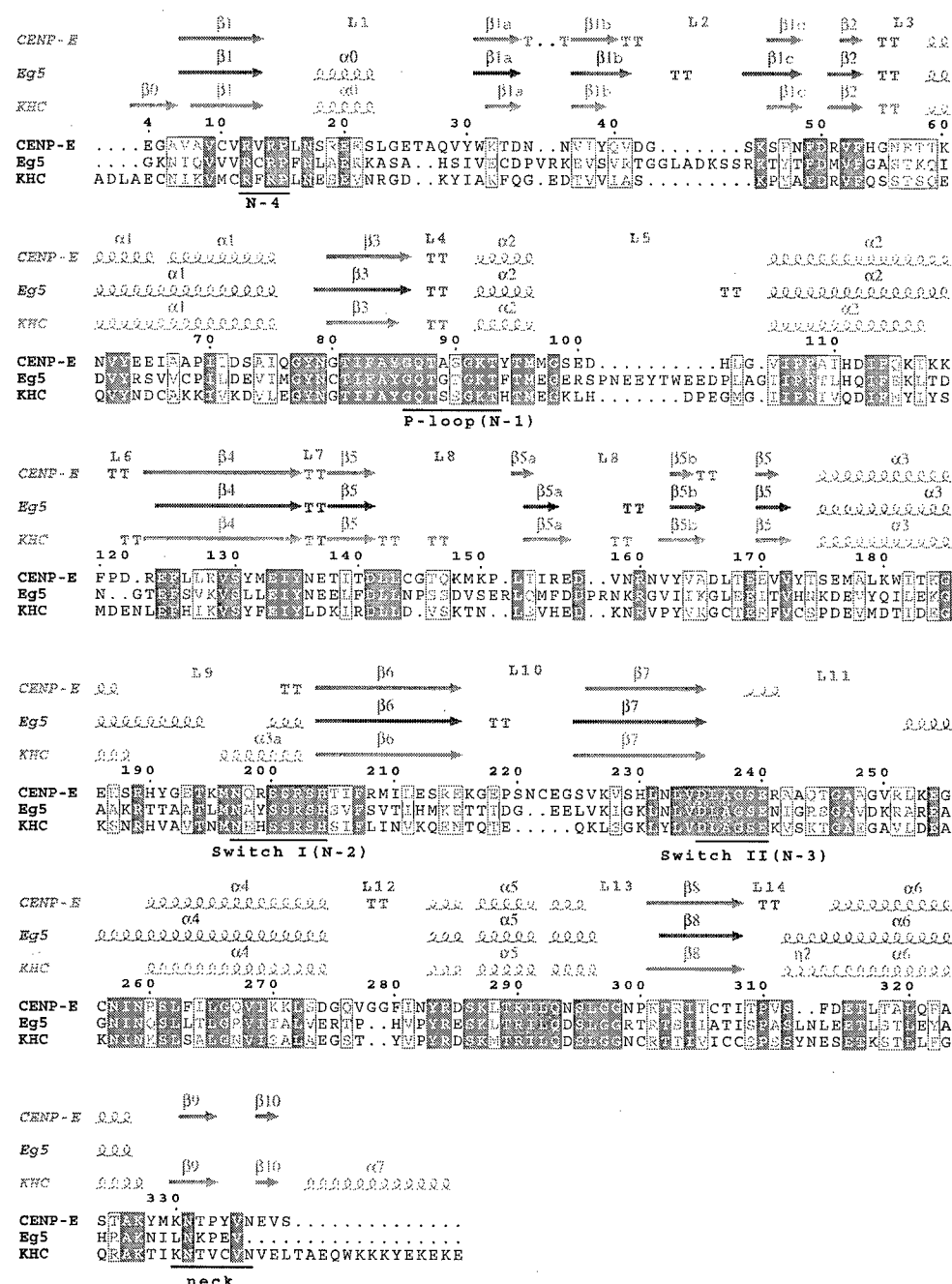


Figure 5. Structural and sequence alignment of the three known human kinesin structures, CENP-E, Eg5 and conventional kinesin. Identical residues are in white on a red background, similar residues are red. The position of the regions forming the nucleotide-binding pocket (N-1 to N-4) and the position of the neck region are underlined in black.

GGA GCC; and CENP-E\_2, 5'-ATA CCT TTT CAG GAG CTC GAG ATC AGT TGA TAC CTC. The PCR product as well as expression vector pET28a were double-digested with NcoI and XhoI and ligated. Positive expression clones were identified by digesting the purified plasmids with the restriction enzymes mentioned above to test for the presence of an insert of the expected size. The sequence was verified by DNA sequencing. Proline 300 was found to be substituted by alanine. The

expression clone codes for the CENP-E motor domain and linker region (residues Met1-Glu342) and eight additional residues (LEHHHHHH) at the C terminus of the protein.

#### Expression and purification of CENP-E

Recombinant CENP-E was expressed and purified as

described for monomeric human Eg5.<sup>43</sup> CENP-E is unstable and consequently the protein was freshly prepared for crystallization assays.

### Protein crystallization

CENP-E in 20 mM Pipes (pH7.3), 200 mM NaCl and 1 mM EGTA was supplemented with 2 mM ATP and 10 mM MgCl<sub>2</sub> and concentrated (AMICON ULTRA-15; 30 kDa) to 11 mg/ml. Insoluble material was removed by centrifugation at 30,000g for 15 minutes. Sitting drops (1 µl protein/1 µl reservoir) at 19 °C were set up with freshly purified protein using a TECAN crystallization robot and 15 commercial kits (Hampton Research). The detailed automated crystallization procedure is described elsewhere.<sup>44</sup> Crystals appeared after two days in different crystallization conditions. Long rods were obtained after manually improving the initial conditions using 1 µl of CENP-E at 11 mg/ml and 1 µl of reservoir solution containing 23% (w/v) polyethylene glycol (PEG) 3350, 0.2 M NaNO<sub>3</sub>, 0.1 M Pipes (pH 7.0), in hanging drops at 19 °C. Crystals belonged to space group *P*2<sub>1</sub> with unit cell parameters *a* = 49.35 Å, *b* = 83.70 Å, *c* = 94.16 Å and monoclinic angle  $\beta$  = 103.05°. The solvent content was calculated to be 42% assuming two molecules per asymmetric unit.

### Data collection

Four different native data sets were collected using an ADSC Quantum-4 CCD detector on beamline ID14-2 at the European Synchrotron Radiation Facility (ESRF). Data were processed with the DENZO/SCALEPACK program suite<sup>45</sup> as well as SCALA from the CCP4 package.<sup>46</sup> The observed diffraction patterns were highly anisotropic with a resolution better than 2.1 Å in one direction but worse in the other. The best dataset yielded data to 2.5 Å resolution with a completeness of 98%. More details of data collection and processing are given in Table 3.

### Structure determination and refinement

The CENP-E motor domain structure was solved by molecular replacement using AMoRe.<sup>47</sup> The structure of conventional human kinesin, Protein Data Bank code 1MKJ<sup>33</sup> without ions, ADP or water molecules was used as a starting model. The correct solution, after performing a two molecule/asymmetric unit search, yielded a correlation coefficient of 39.8% and an *R*-factor of 47.8%. After an initial round of rigid-body refinement, the model was rebuilt manually using TURBO-FRODO.<sup>48</sup> MgADP was included at the initial stages. The model was further refined by cycles of simulated annealing, energy minimization and *B*-factor refinement using CNS<sup>49</sup> and subsequent manual model building. In early stages of refinement, non-crystallographic symmetry restraints with decreasing restraint weights were used, but in the later stages both monomers were considered to be independent. Water molecules were added progressively during refinement. The quality of the model was assessed with PROCHECK.<sup>50</sup> Residues for which no electron density was visible were omitted from the model. In monomer A, residues Lys32, Phe125 and Ser261 were in double conformation. The occupancy of the side-chains of the following residues in monomer B were set to 0.00: Gln115, Lys148, Lys187, Tyr191, Gly192, Glu193, Thr194, Lys195 and Arg202. Residue Tyr39 in

**Table 3.** X-ray data collection and structure refinement of the CENP-E motor domain

|  |   |
|--|---|
| <b>A. Data collection statistics<sup>a</sup></b> |   |
| Unit cell dimensions                             | <i>a</i> = 49.35 Å<br><i>b</i> = 83.70 Å<br><i>c</i> = 94.16 Å<br>$\beta$ = 103.05° |
| Space group                                      | <i>P</i> 2 <sub>1</sub>   |
| Molec./asymmetric unit                           | 2   |
| Max. resolution (Å)                              | 2.5   |
| No of unique reflections                         | 25,698  |
| Overall completeness (%)                         | 98  |
| Last shell completeness (%)                      | 86 <sup>b</sup>   |
| Multiplicity                                     | 4.7   |
| <i>R</i> <sub>sym</sub>                          | 0.064 (0.158) <sup>b</sup>  |
| <b>B. Refinement statistics</b>                  |   |
| No of reflections                                | 24,191  |
| <i>R</i> <sub>working</sub> <sup>d</sup> (%)     | 22.82   |
| <i>R</i> <sub>free</sub> <sup>e</sup> (%)        | 27.87   |
| r.m.s. deviation from ideal                      | Bonds (Å) 0.012<br>Angles (°) 2.08  |

<sup>a</sup> Data collection obtained on the ID14-2 X-ray beamline at the European Synchrotron Radiation Facility (ESRF) in Grenoble (France).

<sup>b</sup> Last resolution shell: 2.64–2.50 Å.

<sup>c</sup>  $R_{\text{sym}} = \sum |I_j - \langle I \rangle| / \sum \langle I \rangle$ , where *I<sub>j</sub>* is the intensity for reflection *j*, and  $\langle I \rangle$  is the mean intensity.

<sup>d</sup>  $R_{\text{working}} = \sum ||F_o| - |F_c|| / \sum |F_c|$ , calculated with the working set.

<sup>e</sup> *R*<sub>free</sub> was similarly calculated with 4.5% of the data excluded from the calculation of *R*<sub>working</sub>.

monomer B was in double conformation. A total of 78.4% of all residues are in most favored, and 16.8% in additionally allowed regions; 0.7% are in disallowed regions. Final refinement statistics are given in Table 3.

### Preparation of Figures

Figures 1 and 3 were prepared using MOLSCRIPT.<sup>51</sup> Figures 2 and 4 were done with BOBSCRIPT.<sup>52</sup> Structural sequence alignment in Figure 5 was performed using the program ESPript<sup>53</sup> and adjusted by hand.

### Data Bank accession numbers

Crystallographic coordinates for the *H. sapiens* CENP-E motor domain structure have been deposited with the RCSB Protein Data Bank under code 1T5C.

### Acknowledgements

We thank Jean-Pierre Andrieu for N-terminal sequencing of human CENP-E and also David Lascoux and Sebastien Brier for MALDI mass spectrometry analysis (IBS, Grenoble). We also acknowledge the help of Ed Mitchel (ESRF Grenoble) during data collection. This work has been funded by grants from the ARC (Association pour la Recherche sur le Cancer, contract number 5197), the CNRS (Centre National de la Recherche Scientifique), the European Union Quality of life Integrated Project SPINE (Structural Proteomics in Europe), contract number QLG2-CT-2002-00988 (to

F.K.) and from the DOD, NIH (GM44762, CA Core grants CA75138 and CA06927) and the Commonwealth of Pennsylvania (to T.Y.).

## References

- Yen, T. J. & Schaar, B. T. (1996). Kinetochore function: molecular motors, switches and gates. *Curr. Biol.* **8**, 381–388.
- Rieder, C. L. & Salmon, E. D. (1998). The vertebrate cell kinetochore and its role during mitosis. *Trends Cell Biol.* **8**, 310–318.
- Grancell, A. & Sorger, P. K. (1998). Kinetochores motor along. *Curr. Biol.* **8**, R382–R385.
- Kapoor, T. M. & Compton, D. A. (2002). Searching for the middle ground: mechanisms of chromosome alignment during mitosis. *J. Cell Biol.* **157**, 551–556.
- Cleveland, D. W., Mao, Y. & Sullivan, K. F. (2003). Centromeres and kinetochores: from epigenetics to mitotic checkpoint signaling. *Cell*, **112**, 407–421.
- Steuer, E. R., Wordeman, L., Schroer, T. A. & Sheetz, M. P. (1990). Localization of cytoplasmic dynein to mitotic spindles and kinetochores. *Nature*, **345**, 266–268.
- Pfarr, C. M., Coue, M., Grissom, P. M., Hays, T. S., Porter, M. E. & McIntosh, J. R. (1990). Cytoplasmic dynein is localized to kinetochores during mitosis. *Nature*, **345**, 263–265.
- Yen, T. J., Compton, D. A., Wise, D., Zinkowski, R. P., Brinkley, B. R., Earnshaw, W. C. & Cleveland, D. W. (1991). CENP-E, a novel human centromere-associated protein required for progression from metaphase to anaphase. *EMBO J.* **10**, 1245–1254.
- Yen, T. J., Li, G., Schaar, B. T., Szilak, I. & Cleveland, D. W. (1992). CENP-E is a putative kinetochore motor that accumulates just before mitosis. *Nature*, **359**, 536–539.
- Wordeman, L. & Mitchison, T. J. (1995). Identification and partial characterization of mitotic centromere-associated kinesin, a kinesin-related protein that associates with centromeres during mitosis. *J. Cell Biol.* **128**, 95–104.
- Wood, K. W., Sakowicz, R., Goldstein, L. S. & Cleveland, D. W. (1997). CENP-E is a plus end-directed kinetochore motor required for metaphase chromosome alignment. *Cell*, **91**, 357–366.
- Yucel, J. K., Marszalek, J. D., McIntosh, J. R., Goldstein, L. S., Cleveland, D. W. & Philp, A. V. (2000). CENP-meta, an essential kinetochore kinesin required for the maintenance of metaphase chromosome alignment in *Drosophila*. *J. Cell Biol.* **150**, 1–11.
- Miki, M., Setou, M., Kaneshiro, K. & Hirokawa, N. (2001). All kinesin superfamily protein, KIF, genes in mouse and human. *Proc. Natl Acad. Sci. USA*, **98**, 7004–7011.
- Dagenbach, E. M. & Endow, S. A. (2004). A new kinesin tree. *J. Cell Sci.* **117**, 3–7.
- Brown, K. D., Coulson, R. M., Yen, T. J. & Cleveland, D. W. (1994). Cyclin-like accumulation and loss of the putative kinetochore motor CENP-E results from coupling continuous synthesis with specific degradation at the end of mitosis. *J. Cell Biol.* **125**, 1303–1312.
- Brown, K. D., Wood, K. W. & Cleveland, D. W. (1996). The kinesin-like protein CENP-E is kinetochore-associated throughout poleward chromosome segregation during anaphase-A. *J. Cell Sci.* **109**, 961–969.
- Schaar, B. T., Chan, G. K., Maddox, P., Salmon, E. D. & Yen, T. J. (1997). CENP-E function at kinetochores is essential for chromosome alignment. *J. Cell Biol.* **139**, 1373–1382.
- Yao, X., Abrieu, A., Zheng, Y., Sullivan, K. F. & Cleveland, D. W. (2000). CENP-E forms a link between attachment of spindle microtubules to kinetochores and the mitotic checkpoint. *Nature Cell Biol.* **2**, 484–491.
- Liu, S. T., Chan, G. K., Hittle, J. C., Fujii, G., Lees, E. & Yen, T. J. (2003). Human MPS1 kinase is required for mitotic arrest induced by the loss of CENP-E from kinetochores. *Mol. Biol. Cell*, **14**, 1638–1651.
- Weaver, B. A., Bonday, Z. Q., Putkey, F. R., Kops, G. J., Silk, A. D. & Cleveland, D. W. (2003). Centromere-associated protein-E is essential for the mammalian mitotic checkpoint to prevent aneuploidy due to single chromosome loss. *J. Cell Biol.* **162**, 551–563.
- McEwen, B. F., Chan, G. K., Zubrowski, B., Savoian, M. S., Sauer, M. T. & Yen, T. J. (2001). CENP-E is essential for reliable bioriented spindle attachment, but chromosome alignment can be achieved via redundant mechanisms in mammalian cells. *Mol. Biol. Cell*, **12**, 2776–2789.
- Liao, H., Li, G. & Yen, T. J. (1994). Mitotic regulation of microtubule cross-linking activity of CENP-E kinetochore protein. *Science*, **265**, 394–398.
- Chan, G. K., Schaar, B. T. & Yen, T. J. (1998). Characterization of the kinetochore binding domain of CENP-E reveals interactions with the kinetochore proteins CENP-F and hBUBR1. *J. Cell Biol.* **143**, 49–63.
- Zecevic, M., Catling, A. D., Eblen, S. T., Renzi, L., Hittle, J. C., Yen, T. J. *et al.* (1998). Active MAP kinase in mitosis: localization at kinetochores and association with the motor protein CENP-E. *J. Cell Biol.* **142**, 1547–1558.
- Endow, S. A. & Fletterick, R. J. (1998). Reversing a “backwards” motor. *BioEssays*, **20**, 108–112.
- Woelke, G. & Schliwa, M. (2000). Directional motility of kinesin motor proteins. *Biochim. Biophys. Acta*, **1496**, 117–127.
- Thrower, D. A., Jordan, M. A. & Wilson, L. (1996). Modulation of CENP-E organization at kinetochores by spindle microtubule attachment. *Cell Motil. Cytoskel.* **35**, 121–133.
- DeLuca, J. G., Newton, C. N., Himes, R. H., Jordan, M. A. & Wilson, L. (2001). Purification and characterization of native conventional kinesin, HSET, and CENP-E from mitotic HeLa cells. *J. Biol. Chem.* **276**, 28014–28021.
- Hirel, P. H., Schmitter, M. J., Dessen, P., Fayat, G. & Blanquet, S. (1989). Extent of N-terminal methionine excision from *Escherichia coli* proteins is governed by the side-chain length of the penultimate amino acid. *Proc. Natl Acad. Sci. USA*, **85**, 8247–8251.
- Kozielski, F., Sack, S., Marx, A., Thormählen, M., Biou, V., Thompson, A. *et al.* (1997). The crystal structure of dimeric kinesin and implications for microtubule-dependent motility. *Cell*, **91**, 985–994.
- Kozielski, F., De Bonis, S., Buhrmeister, W. P., Cohen-Addad, C. & Wade, R. H. (1999). The crystal structure of the minus-end-directed microtubule motor protein ncd reveals variable dimer conformations. *Structure*, **7**, 1407–1416.
- Sack, S., Muller, J., Marx, A., Thormählen, M., Mandelkow, E. M., Brady, S. T. & Mandelkow, E. (1997). X-ray structure of motor and neck domains from rat brain kinesin. *Biochemistry*, **36**, 16155–16165.

33. Sindelar, C. V., Budny, M. J., Rice, S., Naber, N., Fletterick, R. & Cooke, R. (2002). Two conformations in the human kinesin power stroke defined by X-ray crystallography and EPR spectroscopy. *Nature Struct. Biol.* **9**, 844–848.
34. Lombillo, V. A., Stewart, R. J. & McIntosh, J. R. (1995). Minus-end-directed motion of kinesin-coated microspheres driven by microtubule depolymerization. *Nature*, **373**, 161–164.
35. Turner, J., Anderson, R., Guo, J., Beraud, C., Fletterick, R. & Sakowicz, R. (2001). Crystal structure of the mitotic spindle kinesin Eg5 reveals a novel conformation of the neck-linker. *J. Biol. Chem.* **276**, 25496–25502.
36. Wade, R. H. (2002). Sequence landmark patterns identify and characterize protein families. *Structure*, **10**, 1329–1336.
37. Blangy, A., Lane, H. A., d'Herin, P., Harper, M., Kress, M. & Nigg, E. A. (1995). Phosphorylation by p34cdc2 regulates spindle association of human Eg5, a kinesin-related motor essential for bipolar spindle formation *in vivo*. *Cell*, **83**, 1159–1169.
38. Mayer, T. U., Kapoor, T. M., Haggarty, S. J., King, R. W., Schreiber, S. L. & Mitchison, T. J. (1999). Small molecule inhibitor of mitotic spindle bipolarity identified in a phenotype-based screen. *Science*, **286**, 971–974.
39. Bergens, G. *et al.* (2002). Mitotic kinesin-targeted anti-tumor agents: discovery, lead optimization and anti-tumor activity of a series of novel quinazolinones as inhibitors of kinesin spindle protein (KSP). *Meeting abstracts, American Association for Cancer Research*. **3648**, AACR, San Francisco, CA.
40. Johnson, R.K. *et al.* (2002). SB-715992, a potent and selective inhibitor of the mitotic kinesin KSP, demonstrates broad-spectrum activity in advanced murine tumors and human tumor xenografts. *Meeting abstracts, American Association for Cancer research*. **1335**, AACR, San Francisco, CA.
41. Miyamoto, D. T., Perlman, Z. E., Mitchison, T. J. & Shirasu-Hiza, M. (2003). Dynamics of the mitotic spindle—potential therapeutic targets. *Prog. Cell Cycle Res.* **5**, 349–360.
42. Jablonski, S. A., Liu, S. T. & Yen, T. J. (2003). Targeting the kinetochore for mitosis-specific inhibitors. *Cancer Biol. Ther.* **2**, 236.
43. DeBonis, S., Simorre, J. P., Crevel, I., Lebeau, L., Skoufias, D. A., Blangy, A. *et al.* (2003). Interaction of the mitotic inhibitor monastrol with human kinesin Eg5. *Biochemistry*, **42**, 338–349.
44. Garcia-Saez, I., Blot, D., Kahn, R. & Kozielski, F. (2004). Crystallization and preliminary crystallographic analysis of the motor domain of human kinetochore-associated protein CENP-E, using an automated crystallization procedure. *Acta Crystallog. sect. D, Biol. Crystallog.* **60**, 1158–1160.
45. Otwinowsky, Z. & Minor, W. (1997). Processing of X-ray diffraction data collected in oscillation mode. *Methods Enzymol.* **276**, 307–326.
46. Collaborative Computational Project, Number 4 (1994) (1994). The CCP4 Suite: programs for protein crystallography. *Acta Crystallog. sect. D, Biol. Crystallog.* **50**, 760–763.
47. Navaza, J. & Saludjian, P. (1997). AMoRe: an automated molecular replacement program package. *Methods Enzymol.* **276**, 581–594.
48. Roussel, A. & Cambillau, C. (1991). The TURBO-FRODO graphics package. *Silicon Graphics Geometry Partners Directory*, vol. 81, Mountain View, CA.
49. Brünger, A. T., Adams, P. D., Clore, G. M., DeLano, W. L., Gros, P., Grosse-Kunstleve, R. W. *et al.* (1998). Crystallography and NMR system: a new software suite for macromolecular structure determination. *Acta Crystallog. sect. D, Biol. Crystallog.* **54**, 905–921.
50. Laskowski, R., MacArthur, M., Moss, D. & Thornton, J. (1993). PROCHECK: a program to check the stereochemical quality of protein structures. *J. Appl. Crystallog.* **26**, 91–97.
51. Kraulis, P. J. (1991). MOLSCRIPT: a program for producing both detailed and schematic plots of protein structures. *J. Appl. Crystallog.* **24**, 946–950.
52. Esnouf, R. M. (1999). Further additions to MolScript version 1.4, including reading and contouring of electron-density maps. *Acta Crystallog. sect. D, Biol. Crystallog.* **55**, 938–940.
53. Gouet, P., Courcell, E., Stuart, D. I. & Metoz, F. (1999). ESPript: multiple sequence alignments in PostScript. *Bioinformatics*, **15**, 305–308.
54. Kull, F. J., Sablin, E. P., Lau, R., Fletterick, R. J. & Vale, R. D. (1996). Crystal structure of the kinesin motor domain reveals a structural similarity to myosin. *Nature*, **380**, 550–555.

Edited by R. Huber

(Received 2 February 2004; received in revised form 7 May 2004; accepted 12 May 2004)

## Chapter 4.3

# MITOTIC CHECKPOINT, ANEUPLOIDY AND CANCER

Tim J. Yen<sup>1</sup> and Gary D. Kao<sup>2</sup>

<sup>1</sup> Fox Chase Cancer Center, Philadelphia, USA; <sup>2</sup> Dept of Radiation Oncology, University of Pennsylvania, Philadelphia, USA

## 1. INTRODUCTION

The mitotic checkpoint is a failsafe mechanism that prevents cells with unaligned chromosomes from prematurely exiting mitosis. As chromosome instability (CIN) and aneuploidy are features common amongst many cancers, the mitotic checkpoint may play a pivotal role in promoting tumorigenesis. The discovery of an evolutionarily conserved set of mitotic checkpoint genes has stimulated efforts to examine their importance in the origin of cancer and their use in potential new therapies for cancer.

The transformation of a normal cell into a malignant tumour is a multi-step process that cannot be accounted for by spontaneous mutations that arise from the inherent error rates that are associated with DNA replication and repair. Indeed, it has been estimated that the natural mutation rate is so low that it cannot generate enough mutations for cancer to develop within a human lifespan (Loeb, 1991; Orr-Weaver and Weinberg, 1998). That a majority of human cancers exhibit gross chromosome abnormalities and gene mutations strongly suggests that carcinogenesis is driven by mechanisms that actively destabilise the genome. Microsatellite instability (MIN) is one such mechanism whereby increased mutation rate at the nucleotide level is attributed to defects in DNA mismatch repair genes (Lengauer et al., 1998). Chromosome instability (CIN) is a second mechanism that promotes genome instability through the loss or gain of chromosomes. Indeed, many types of tumours are aneuploid and *in vitro* studies of colorectal cancer cell lines have shown a defect in maintaining a stable karyotype (Cahill et al., 1998; Pihan and Doxsey, 1999; Takahashi et al., 1999). Only recently have there been mechanistic advances in understanding the molecular basis for CIN. These insights came to light

largely from a convergence of genetic and biochemical studies of the mitotic checkpoint, a failsafe mechanism that prevents aneuploidy by ensuring that cells with even a single unaligned chromosome cannot exit mitosis. This chapter will review our current knowledge of the mitotic checkpoint and examine its relationship with tumorigenesis.

## **2. CHROMOSOME SEGREGATION**

### **2.1 Kinetochore Functions**

The kinetochore is a macromolecular complex that is localised at the centromeres of chromosomes where it plays an essential role in mediating attachment of the chromosome to the spindle. Kinetochores interact with microtubules differently than other organelles (i.e. vesicles) in that they bind to the highly dynamic plus ends of microtubules, rather than along the side or the lattice of the microtubule (Rieder and Salmon, 1994). Thus, unlike organelles that rely on motors to translocate them along a static microtubule surface, the motility of chromosomes is specified by the kinetochore's ability to remain attached to the end of a microtubule that is rapidly switching between elongating and shortening states. How this is achieved is not clear but is likely to be specified by the combined and coordinated activities of a plethora of microtubule binding proteins and molecular motors that localise to kinetochores (Biggins and Walczak, 2003). Despite the large numbers of microtubule binding proteins at kinetochores, microtubule connections are established by chance encounters that depend on the location of the chromosome relative to the spindle. Chromosomes situated near the centre of the spindle rapidly establish bipolar connections as both kinetochores encounter microtubules at a high frequency. Chromosomes situated near a pole will rapidly establish a monopolar attachment but attachment to the opposite pole requires significantly more time as the frequency at which they encounter microtubules from the opposite pole is low.

As with many situations that rely on chance, there is the potential for mistakes. Kinetochores are not an exception as they can establish non-productive interactions as in cases when both kinetochores are connected to the same pole or one kinetochore is connected to microtubules from both poles and combinations of the two. These aberrant connections, if unresolved, can lead to chromosome fragmentation or nondisjunction (Cimini et al., 2001).

## 2.2 The Mitotic Checkpoint

The stochastic and error-prone nature by which chromosomes establish connections to the spindle explains why chromosomes cannot achieve metaphase alignment synchronously (Nicklas, 1997; Nicklas and Ward, 1994). The cell is therefore confronted with the problem of knowing when all of its chromosomes are aligned before it decides to proceed into anaphase. This problem is solved by the mitotic checkpoint which is a failsafe mechanism that monitors kinetochore microtubule attachments so that a single defective kinetochore will delay the onset of anaphase. In order to satisfy this checkpoint, kinetochores must be fully saturated with microtubules (~25 microtubules per kinetochore for mammals) and sufficient tension develops between sister kinetochores as a result of opposing poleward forces that attempt to pull apart the sister chromatids. If either of these parameters is not fulfilled, the checkpoint must then execute a program that inhibits mitotic exit. This program can be envisioned as a signalling cascade whereby a localised defect at a single kinetochore alters the global biochemical status of the cell. The nature by which the kinetochore generates the "wait anaphase" inhibitory signal is not entirely clear. However, the target of the "wait anaphase" signal is the Anaphase Promoting Complex/Cyclosome (APC/C) (Skibbens and Hieter, 1998); an E3 ubiquitin ligase that promotes the degradation of key proteins to irreversibly drive cells from metaphase to anaphase (King et al., 1995; Sudakin et al., 1995). Thus, the mitotic checkpoint is a highly complex program that consists of multiple modules, defects in any of its components will result in chromosome instability that promotes tumorigenesis.

### 2.2.1 Mitotic Checkpoint Proteins Monitor Kinetochore Attachments

The molecular components of the mitotic checkpoint are specified by a collection of evolutionarily conserved genes that include Mad1, Mad2, Mad3 (BubR1), Bub1, Bub3 and Mps1 (Musacchio and Hardwick, 2002). With the exception of Mps1, Bub1 and BubR1, which are protein kinases, the biochemical functions of the remaining proteins are not well understood. Cytological studies have shown that all of these proteins bind to kinetochores and are thus likely to be involved in monitoring attachments or generating the "wait anaphase" signal. In the case of Mad1 and Mad2, their preferential localisation at unattached kinetochores (Chen et al., 1996; Li and Benezra, 1996; Waters et al., 1998) suggests that they may be part of a counting mechanism that monitors microtubule occupancy and contributes to the generation of the "wait anaphase" signal. As kinetochores become saturated with microtubules, these proteins are released and the checkpoint signalling is silenced.

The existence of a tension-sensitive checkpoint was first demonstrated in insect spermatocytes where application of an external force to the

unattached kinetochore of a monopolar chromosome would relieve the checkpoint induced delay in meiosis (Li and Nicklas, 1995). The spermatocytes proceeded into anaphase because the external force exerted tension that would normally be applied by microtubule attachments. Although this result was inconsistent with the idea that checkpoint is silenced only when both kinetochores are saturated with microtubules and develop tension, this discrepancy may be attributed to the difference between mitotic versus meiotic systems. Evidence supporting a tension-sensitive checkpoint in somatic cells has come from experiments that examined the mechanism by which the anti-cancer drug, Taxol arrests mammalian cells in mitosis (Waters et al., 1998). Cells treated with Taxol are able to establish a full complement of kinetochore microtubule attachments. However, tension did not develop because the drug suppressed microtubule dynamics that normally contributed to the generation of poleward force. As the vast majority of the bipolar attached kinetochores lacked detectable Mad2, it suggested that Mad2 does not respond to loss of tension and that other components were maintaining the checkpoint arrest. Bub1 and BubR1 (Bub1-related) kinases are candidates as they are present at kinetochores with reduced tension (Skoufias et al., 2001). However, it is important to point out that unlike Mad2, neither of these proteins completely dissociate from kinetochores of aligned chromosomes (Hoffman et al., 2001). Thus, their presence alone cannot be used as an indicator of whether the checkpoint is active.

### **2.2.2 Tension Sensing helps Resolve Aberrant Kinetochore Attachments**

The importance of a tension-sensitive checkpoint is not to merely allow cells to arrest in response to microtubule poisons such as taxol. The need arises because kinetochores can form aberrant attachments where both sister kinetochores are attached to the same pole (syntelic) or the same kinetochore is attached to both poles (merotelic). In both instances, kinetochores are fully saturated with microtubules but lack tension (Cimini et al., 2001). Clearly, if microtubule occupancy was the only criterion that is used by the checkpoint, these aberrant connections would go unchecked and thus lead to non-disjunction or broken chromosomes. Recent studies in both yeast and human cells indicate that the aurora B/Ipl1 kinase is responsible for monitoring tension in order to resolve merotelic and syntelic attachments (Ditchfield et al., 2003; Hauf et al., 2003; Tanaka et al., 2002). How aurora B responds to lack of tension is unclear but it is thought to stimulate the release of microtubules by regulating the microtubule depolymerase activity of the kinesin-like MCAK protein (Andrews et al., 2004; Lan et al., 2004). Despite these intriguing findings, there is uncertainty as to whether aurora B indeed defines the tension-sensitive arm of the mitotic checkpoint as it may be part of an elaborate self-correcting mechanism (Andrews et al., 2003). That aurora B is essential for taxol-induced mitotic arrest may result from an



indirect action on the checkpoint (Ditchfield et al., 2003; Hauf et al., 2003). The mitotic checkpoint may be responding not directly to loss of tension but rather to the presence of detached kinetochores that are induced by aurora B. This possibility is consistent with the observation that there are always a few kinetochores that retain Mad2 in Taxol arrested cells (Waters et al., 1998).

### 2.2.3 The Anaphase Promoting Complex is the Target of the Mitotic Checkpoint

There are two models proposed to explain how defective kinetochores can inhibit APC/C activity (Chan and Yen, 2003). In the "Sequestration Model" a dynamic pool of Mad2 cycles through unattached kinetochores where it is proposed to undergo a conformational change that increases its affinity for Cdc20, a WD repeat protein, that normally recruits substrates to the APC/C. In vitro, Mad2 can bind Cdc20 and prevent it from activating the APC/C (Fang et al., 1998). Structural studies showed that Mad2 undergoes a major conformational change when bound to Cdc20 or to its other partner, Mad1 (Luo et al., 2000; Luo et al., 2004). *In vivo*, Mad2 has been shown to cycle rapidly through kinetochores at approximately 2000 molecules per minute (Howell et al., 2000). How Mad2 exchanges its partner between Mad1 at the kinetochores and Cdc20 in the cytosol remains a challenging problem. Clarification of this issue may address the more important question as to what the fate of Mad2 is after release its release from kinetochores.

The alternative model posits that there are two distinct steps to the inhibition of the APC/C. This model came about through the biochemical purification of a factor from HeLa cells that inhibited mitotic APC/C (Sudakin et al., 2001). The Mitotic Checkpoint Complex (MCC) consisting of BubR1, Bub3, Cdc20 and Mad2 forms independently of kinetochores and is thus not the "wait anaphase" signal. MCC exists in near stoichiometry with APC/C in HeLa cells and is the only known inhibitor of APC/C that is purified from mitotic cells. It is proposed that a preformed pool of MCC in interphase provides cells with a rapid way to inhibit the APC/C when it is activated upon entry into mitosis. The affinity of these two complexes for each other cannot be very high as inhibition of the APC/C must be readily reversible to allow cells to exit mitosis. The duration of the MCC/APC/C interaction may be extended if there are unattached kinetochores. In this case, the "wait anaphase" signal is postulated to directly act on the APC/C to sensitise it to prolonged inhibition by the MCC.

The ability to directly test the two-step model *in vivo* is challenging as the same proteins (BubR1, Bub3, Cdc20, Mad2) are involved in both steps. However, two recent reports provided *in vivo* evidence that Mad2 may have kinetochore dependent and independent roles in the mitotic checkpoint. HeLa cells depleted of the kinetochores proteins HEC1/Ndc80 (Martin-Lluesma et al., 2002) or CENP-I, accumulate unaligned chromosomes and delay in mitosis (Liu et al., 2003) et al.,). Surprisingly, this delay occurred

despite the loss of Mps1, Mad1 and Mad2 from kinetochores. This finding was inconsistent with studies where direct inhibition of Mad2 not only abrogated the mitotic checkpoint but accelerated cells out of mitosis before chromosomes could align properly (Gorbsky et al., 1998; Meraldi et al., 2004; Shannon et al., 2002). This discrepancy could be resolved if one argued that cells lacking Mad2 at kinetochores were able to delay in mitosis through the kinetochore-independent mechanism. Indeed, both studies demonstrated that the delay was still dependent on Mad2 even though it had been depleted from kinetochores. It is therefore likely, that this Mad2-dependent delay reflected the action of the MCC. The caveat of both studies is the degree to which Mad2 was depleted from kinetochores. In CENP-I depleted cells, there was a twenty-fold reduction while a subsequent study of HEC1 depleted cells showed about five-fold reduction (DeLuca et al., 2003). As there can be a hundred-fold difference in the level of Mad2 between unattached and fully attached kinetochores (Hoffman et al., 2001), it is possible that the reduction achieved by HEC1 and CENP-I depletion was insufficient to completely silence the production of the "wait anaphase" signal. However, the reduction of Mad2 at kinetochores likely reduced the output of the "wait anaphase" signal as a prolonged mitotic arrest could not be attained when there were only a few unattached kinetochores (Liu et al., 2003). Only when the number of unattached kinetochores was increased was a prolonged delay achieved. As other checkpoint proteins such as BubR1 and Bub1 kinases remained at kinetochores in these cells, it is likely that they were producing the "wait anaphase" signal when Mad2 levels were reduced. However, a threshold level of "wait anaphase" signal was not achieved to sustain a prolonged inhibition of the APC/C.

#### 2.2.4 Spatial and Temporal Regulation of APC/C

The mitotic checkpoint models presented here do not explain two important observations. The degradation of cyclin A, like cyclin B, depends on Cdc20 and APC/C (Geley et al., 2001). Yet, cyclin A is degraded early in prometaphase and is not inhibited when cells are delayed in mitosis (den Elzen and Pines, 2001). The simplest explanation is that the mitotic checkpoint consists of additional layers that may directly act on APC/C substrates. Our current understanding of the mitotic checkpoint also cannot account for how spatial control of APC/C is achieved. Using GFP-cyclin B as a real-time reporter for APC/C activity (Clute and Pines, 1999), it was clear that APC/C does not appear to be activated throughout the cell upon achieving metaphase. Interestingly, GFP-cyclin B that was localised over the spindle was preferentially lost from the pole towards the chromosomes. While this observation supports the idea that checkpoint inhibition of the APC/C may be spatially confined to the spindle, an alternative explanation is that the sensitivity of APC/C substrates may be spatially regulated. This possibility may also account for why cyclin A is insensitive to checkpoint inhibition.

### 2.2.5 Factors that Influence the Mitotic Checkpoint

Genetic studies in mice illustrate an important concept about the mitotic checkpoint. Mice that are haplodeficient for a variety of mitotic checkpoint genes (see below) are viable and grow to adulthood with minimal problems. However, mouse embryo fibroblasts (MEF's) derived from these animals exhibit increased rates of chromosome loss that would seem to be incompatible with normal development. This paradox could be resolved if one considers that the mitotic checkpoint is not an essential process. Cells only need the checkpoint when their chromosomes encounter problems with attaching to the spindle. One could imagine that if the spindle in mouse embryos was highly efficient at capturing chromosomes, they may well tolerate a reduction (not elimination) in their capacity to delay mitosis in face of attachments defects. Indeed, the early embryonic cell cycle of *Drosophila* and *Xenopus* are not subject to mitotic checkpoint control. The situation may be different in mice as homozygous checkpoint mutants are lethal. The variable nature by which different cell types rely on the mitotic checkpoint is ultimately due to the complex interplay amongst components of the spindle, checkpoint proteins, the APC/C and its substrates. The biochemical activities of each of these processes must balance each other to achieve coordination between chromosome alignment and mitotic exit. For example, a moderate overexpression of Cdc20 in budding yeast can drive cells prematurely out of mitosis (Pan and Chen, 2004). The focus on profiling just the mitotic checkpoint proteins in cancer cells may be inadequate to address the origin of their aneuploidy.

If we were to consider the kinetochore, underexpression of a component that is important for microtubule capture would impose demands on the mitotic checkpoint that must be capable of inhibiting all APC/C in the cell. CENP-E is a kinetochore associated kinesin-like protein (McEwen et al., 2001; Schaar et al., 1997; Yao et al., 2000) and its loss causes cells to accumulate monopolar chromosomes and thus delay mitotic exit. Although CENP-E is an essential gene in mice, haplodeficient mice are viable (Putkey et al., 2002; Weaver et al., 2003). However, MEF's derived from these mutant mice showed that they cannot sustain a prolonged mitotic arrest but exited mitosis after a transient delay (Weaver et al., 2003). While one interpretation is that CENP-E is a component of the checkpoint, the explanation lies in its interactions with other kinetochores proteins. Comparison between haplodeficient versus wild type MEF's showed that the levels of BubR1, Mad1 and Mad2 at kinetochores of CENP-E depleted MEF's were reduced by up to 50%. This outcome is similar to that reported when Hela cells were depleted of the kinetochore proteins Hec1 and CENP-I. Their loss led to reduction in the amounts of Mps1, Mad1 and Mad2 at kinetochores. Consequently, these kinetochores cannot generate sufficient amounts of the "wait anaphase" signal to sustain prolonged inhibition of the APC/C. The theme that emerges from the three studies is that unattached

kinetochores can vary their production of “wait anaphase” signal depending on the amount or activities of the checkpoint proteins present there.

Adenomatous polyposis coli (APC) is a tumour suppressor gene that is frequently mutated in colorectal carcinomas. While APC is well recognised for its role in the Wnt signalling pathway, recent studies have shown that it is important for kinetochore microtubule attachments (Fodde et al., 2001; Kaplan et al., 2001). APC was found at the tips of microtubules that are attached to kinetochores. Furthermore, it was found to form a complex with checkpoint proteins Bub1 and Bub3 (Kaplan et al., 2001). Significantly, expression of mutant APC diminished the mitotic checkpoint response of once checkpoint proficient cells (Tighe et al., 2001). Thus, the combination of defective kinetochore attachments and a reduced mitotic checkpoint in cells expressing mutant APC is likely to result in aneuploidy in colorectal cancers.

These situations underscore two important points. First, disruption of the mitotic checkpoint does not occur exclusively by mutating the bona fide checkpoint genes. Mutations that alter any component that feeds into the pathway can influence the mitotic checkpoint. Second, the mitotic checkpoint is not simply an on/off switch as its capacity to delay mitosis varies as a function of complex interactions with the kinetochore and the APC/C. That cells can exhibit variable lengths of delay suggests that the ratio between the “wait anaphase” signal and its target, the APC/C, is an important parameter in dictating how long a cell can delay mitosis in response to unaligned chromosomes.

### **3. MITOTIC CHECKPOINT, ANEUPLOIDY AND CANCER**

#### **3.1 Genetic Evidence in Human Cancers**

The identification of mitotic checkpoint genes has contributed significantly towards a molecular understanding of aneuploidy, and mechanisms that might be associated with increased carcinogenesis. Interest in such mechanisms is underscored by the recent identification of mutations in *Bub1B*, the gene encoding the BubR1 protein, in families with mosaic variegated aneuploidy (MVA) (Hanks et al, 2004). MVA is a rare autosomal recessive disorder marked by a high predisposition to mitotic non-disjunction, the probable cause of the high levels of aneuploidy of multiple different chromosomes and tissues in each affected individual. The phenotype of this condition has been quite consistent in cases reported to date, and which has included severe microcephaly, growth deficiency, mild physical anomalies, eye anomalies and mental retardation. The risk of malignancy seems to be elevated, and have included rhabdomyosarcoma,

Wilms tumour, and leukemia Hanks et al. assessed eight pedigrees with MVA, and identified biallelic mutations in *Bub1B* in five families. In all cases, mutations in one allele results in the inactivation of the gene while missense mutations were found in the second allele. Four of the five missense mutations occurred in the catalytic domain and thus suggest a dysfunctional BubR1 kinase. The fifth missense mutation was found in a region of the protein with no ascribed function. Nevertheless, this missense mutation along with one found in the kinase domain were associated with two cases of embryonal rhabdomyosarcoma. Why only two cases of cancer were identified amongst the five MVA families is unclear but suggests additional factors are likely to be involved in the cancer development.

The MVA study was predated by one of the first studies to draw attention to a potential role for perturbed mitotic checkpoint function in the etiology of human cancer (Cahill et al., 1998). Heterozygous mutations in Bub1 and BubR1 kinases were found in a few of the nineteen aneuploid colorectal cancer cell lines that were examined. Although the BubR1 mutations were not pursued, the effects of the Bub1 mutants were examined in more detail. In V400 cells, a mutation at an intronic splice donor site created a frameshift mutation that led to a premature termination codon. In V429 cells, a missense mutation that converted a serine to a tyrosine was identified. When the Bub1 mutants were transfected into a checkpoint proficient colorectal cancer cells (HCT116), the transfectants were no longer able to block mitosis when challenged with spindle poisons. It was therefore concluded that these were dominant mutants that were responsible for the defective checkpoint response of the V400 and V429 cells. The caveat is that this result was obtained by overexpressing the mutant proteins to non-physiological levels. It is therefore unclear if the amount of mutant proteins expressed in the V400 and V429 cells can effectively compete against the wild type protein.

Since that report, there have surprisingly few reports of mutated mitotic checkpoint genes in human cancers cell lines, or cancers freshly biopsied or resected from patients in the clinic. For example, no mutations in either Bub3, BubR1 or Bub1 were found in a large number of glioblastomas and lung cancers derived from patients or cell lines (Reis et al., 2001; Sato et al., 2000). One sample from a series of surgically resected colorectal, hepatocellular, and renal tumours was found to contain a missense mutation in Bub1 (Shichiri et al., 2002). Whether this mutation disrupted checkpoint function of the protein is unknown. However, quantitation of transcript levels by real-time polymerase chain reaction identified a subset of tumours with depressed levels of mRNA that was postulated to be due to epigenetic silencing of the genes. This subset of tumours was associated with a significantly higher recurrence rate, suggesting that low levels of expression of BubR1 or Bub1 might confer a growth advantage to the tumours of the subset. Examples of heterozygous mutations in the Bub1 gene have been reported in T lymphoblastic leukemia cell lines and in patients with acute lymphoblastic leukemia (ALL) and Hodgkin's lymphoma (Ru et al., 2002).

Of five patient samples examined, three were found to harbour deletion mutations in Bub1. A similar study of adult T-cell leukemia (ATLL) that exhibited aneuploidy showed that in 4 out of 10 cases, mutations in either Bub1 and BubR1 were found (Ohshima et al., 2000). All except one mutation, which resulted in a truncated BubR1, were mutations that resulted in an amino acid substitution. It remains to be seen if the biochemical functions of these mutant proteins were affected.

The search for Mad1 and Mad2 mutations also showed that they did not occur at high frequency. A screen for Mad1 mutations involving a large panel of 44 cancer cell lines and 133 primary tumours consisting of lymphomas, bladder, breast and gliomas identified only eight mutations that potentially disrupted Mad1 function (Tsukasaki et al., 2001). Two of the eight mutations resulted in premature termination while the other six mutations led to amino acid substitutions. A study of Mad2 in a group of 96 human primary tumours comprised of 44 transitional-cell carcinomas of the bladder, 42 adult soft-tissue sarcomas and 10 hepatocellular carcinomas identified one missense mutation in a bladder tumour where an isoleucine was mutated to a valine (Hernando et al., 2001). This alteration did not appear to alter protein function as transfection of the mutant Mad2 cDNA into cells did not result in a phenotype different from wild type cDNA. Similar screens have shown that Mad2 mutations are rare in cancer cells obtained from breast, lung (Gemma et al., 2001; Percy et al., 2000; Takahashi et al., 1999), and digestive tract (Imai et al., 1999). However, reduced expression of Mad2 protein and mRNA has been reported in breast (Li and Benezra, 1996; Percy et al., 2000), nasopharyngeal and ovarian cancer cell lines (Wang et al., 2002; Wang et al., 2000) that exhibited a defect in their mitotic checkpoint response to spindle poisons. The molecular explanation for why some cancer cells do not express sufficient levels of Mad2 remains unknown but illustrates the earlier point that inactivation of the mitotic checkpoint can be achieved in many different ways.

### 3.1.1 Mutations in Mitotic Checkpoint Genes are Rare

It may be premature to conclude from these studies whether disruption of the mitotic checkpoint genes promotes tumorigenesis. As many of the studies did not exhaustively screen all of the known checkpoint genes, it is possible that mutations may still be found. However, one study that examined all of the known checkpoint genes in nineteen aneuploid cell lines did not uncover any mutations (Cahill et al., 1999). In these cases, the mitotic checkpoint defects may be due to mutations that affect other components (spindle, kinetochore, APC/C and its substrates) that influence the mitotic checkpoint. Of the mutations that have been identified in the mitotic checkpoint genes, the majority are missense mutations whose effects on the stability or biochemical activity of the protein is not known. Western blots to determine the expression levels of various checkpoint proteins

would be very informative. Equally informative are immunocytological assays that monitor the localisation at kinetochores of key mitotic checkpoint proteins. In the case of Bub1, we now know that it is important for assembling other proteins to the kinetochore (Johnson et al., 2004). Those proteins may be informative biomarkers that indirectly monitor Bub1 activity. Similarly, the localisation of Mad2 at kinetochores may be an informative biomarker for mitotic checkpoint status. These immunocytological assays are not only a simple way to functionally assess mutant checkpoint genes, it may be quite effective in screening for the molecular defects in cells that are phenotypically defective for the mitotic checkpoint. The immunocytological data may help to define the pathways that are affected in these cells.

### 3.2 Mouse Models that Test the Link between Aneuploidy and Cancer

Efforts to directly test the link between aneuploidy and tumorigenesis have been to conduct targeted disruption of mitotic checkpoint genes in mice. A strikingly consistent finding has been that mice with targeted knockouts of these genes are nonviable, dying early in embryogenesis. To circumvent the early lethality of the total knockouts, partial knockouts have been generated, in which the mice are haplodeficient for genes encoding the mitotic checkpoint proteins (Table 1).

Table 1. Characteristics of Mice Deficient for Mitotic Checkpoint Genes

| Gene Target                          | BubR1                                       | Bub1  | Mad2   | Bub3/Rae1                            |
|--------------------------------------|---|---|--|--------------------------------------|
| Genotype                             | +/-   | h/h <sup>1</sup>  | +/-  | +/-                                  |
| Expression                           | Reduced                                     | Much reduced  | Reduced  | Reduced                              |
| Checkpoint                           | Loss  | Loss  | Loss   | Loss                                 |
| Aneuploidy in MEF's                  | Yes   | Yes   | Yes  | Yes                                  |
| Spontaneous tumours in young animals | No  | No  | No   | No                                   |
| Tumour formation during lifespan     | Carcinogen induced lung and colonic tumours | 5% of moribund or deceased animals have solitary tumour | Lung tumours in minority of animals after long latency | Carcinogen induced lung tumours only |
| Other phenotypes                     | NA <sup>2</sup>                             | Early aging, Shortened lifespan.                        | NA   | NA                                   |

<sup>1</sup> hypomorphic

<sup>2</sup> Not Assessed

A number of other common themes have emerged between the efforts targeting different proteins:

- Haplodeficient MEFs show reductions of 25-75% in the expressed levels of the targeted proteins, indicating that the remaining allele does not fully compensate for the missing allele.
- The reduction in expressed protein is sufficient to inactivate the mitotic checkpoint in response to microtubule disruption (e.g. by nocodazole).
- Haplodeficient MEFs show increased aneuploidy at the earliest stages post-coitus when they were harvested.
- Haplodeficient mice are phenotypically normal in utero, survive birth, and grow well into adulthood, during which their body mass is similar to wildtype mice.
- No spontaneous tumour formation (except for papillary lung cancers late in life of Mad2-haplodeficient mice).

### 3.2.1 Mad2

Mad2 null mice die 6.5 days after coitus (Dobles et al., 2000), while Mad2 haplodeficient mice are viable well into adulthood. Mouse embryo fibroblasts (MEFs) from the Mad2 haplodeficient mice were found on metaphase spread analysis to have a high frequency of cells with premature sister chromatid separation (30-57% of cells), and a likewise high proportion of cells that were aneuploid (33-60%), suggesting a link between the chromosomal missegregation and development of aneuploidy. Despite the high proportion of aneuploidy in embryonic cells, animals were not found to have early spontaneous tumour development, and live comparatively long lifespans. Upon sacrifice at 18-19 months, 14/57 (27%) of Mad2-deficient animals were found to have papillary lung tumours, a tumour that is extremely rare in wildtype animals. No increased incidence of lymphomas or other tumours were noted in the haplodeficient animals.

### 3.2.2 Bub3 and Rae1

Rae1 is a member of the superfamily of WD proteins that is most similar to Bub3. Findings that included interactions between Rae1 and Bub1 in cultured cells suggested it may be involved in the mitotic checkpoint (Wang et al., 2001). Targeted deletion of either Bub3 or Rae1 in mice showed that they were essential genes as homozygous Bub3 and Rae1 null mutants died by days E8.5 and E5.5, respectively (Babu et al., 2003). Rae1 haplodeficient mice were viable and survived to adulthood. MEFs derived from Rae1 +/- mice exhibited increased aneuploidy relative to wildtype MEFs. Nevertheless, spontaneous tumours were not detected in the animals. Similar to the Rae1-haplodeficient MEFs, the Bub3-haplodeficient MEFs were deficient for the nocodazole-induced mitotic arrest and showed increased aneuploidy. Retroviral-mediated gene-transfer of full-length Rae1 cDNA into both Rae1- and Bub3-haplodeficient MEFs restored the



nocodazole-induced mitotic checkpoint. To further assess the relationship between Rael and Bub3, mice haplodeficient for both genes were generated. MEFs derived from embryos that were haplodeficient for both Rael and Bub3 showed considerably greater aneuploidy than either targeted haplodeficient MEF alone. Despite the increased rates of aneuploidy of the compound heterozygote MEF's, the mice were viable and showed no reduced body mass or spontaneous tumour formation. Lung tumours were obtained only after the animals were exposed to a potent carcinogen from an early age. The frequency of tumours was: WT: 50%, Bub3 +/-: 72%, Rael +/-: 80%, Bub3 +/- Rael +/-: 90%. Thus, partial abrogation of Rael and Bub3, either separately or together, did not result in increased spontaneous tumour formation. A notable increase in the proportion of animals with tumours was only seen after exposure to a potent carcinogen.

### 3.2.3 BubR1

Targeted deletion of BubR1 in mice have shown that this is also an essential gene for embryogenesis (Baker et al., 2004; Dai et al., 2004). Analysis of haplodeficient BubR1 MEF's isolated at day E14.5 showed that they expressed only about 25%, not the expected 50%, of the level of BubR1 protein compared to wildtype BubR1 +/+ MEFs. The BubR1 heterozygous MEF's are haploinsufficient as they failed to arrest in mitosis in response to nocodazole. Despite the loss of the mitotic checkpoint, no spontaneous tumours were identified in any of the heterozygous mice. Application of a potent colonic carcinogen resulted in a higher average number of colonic microadenomas, adenomas, and adenocarcinomas in the BubR1 haplodeficient mice compared to wildtype mice (the proportion of haplodeficient animals which became afflicted with these tumours was not stated). Other major organs were also searched for tumour formation, and only the lung and liver showed tumours (the incidence and average number of these tumours per mouse was not stated).

A fascinating aspect of these animal studies is that the level of expression of the mitotic checkpoint proteins appears to dictate in a dramatic fashion the resulting cellular phenotype and embryonic development. Complete absence of expression of these proteins as in the homozygous knockouts is incompatible with embryonic development. Partial expression (levels of protein that are 25-50% of wildtype cells) of protein in the haplodeficient animals is insufficient to mediate the mitotic checkpoint in response to microtubule-disrupting drugs, yet it enables normal development, birth, and growth, including well into adulthood. Even a reduction in the dosage of a checkpoint protein can be tolerated as long as the cells can delay for sufficient amounts of time for chromosomes to align properly.

The importance of dosage was demonstrated dramatically in a study of mice that were engineered to allow for graded expression of BubR1 (Baker et al., 2004). This was accomplished by crossing mice with alleles for *Bub1b* (encoding for BubR1 protein) that were knockout (*Bub1b*),

hypomorphic (*Bub1b*<sup>H</sup>), or wildtype (*Bub1b*<sup>+</sup>). MEFs were generated that expressed no BubR1 protein (*Bub1b*<sup>-/-</sup>), extremely low levels (4% of wildtype) (*Bub1b*<sup>-H</sup>), or very low levels (11% of wildtype) (*Bub1b*<sup>H/H</sup>), and finally low levels of protein. *Bub1b*<sup>H/+</sup> and *Bub1b*<sup>-/+</sup> MEFs showed protein levels respectively 29% and 42% of wildtype MEFs.

Interestingly, *Bub1b*<sup>-H</sup> (4% of wild type) mice developed unimpeded, but died within several hours of birth of respiratory failure, suggesting deficient development of some tissue that is critical to maintain respiratory fitness. This observation indicates that specific organ systems might have different thresholds of BubR1 protein expression to ensure sufficient development and growth. In contrast, *Bub1b*<sup>H/H</sup> mice showed slow postnatal growth, but survived to adulthood. Finally, the *Bub1b*<sup>H/+</sup> and *Bub1b*<sup>-/+</sup> mice both showed no discernable abnormal phenotype. The level of BubR1 protein expression that was sufficient to ensure development and growth to adulthood could therefore be established as between 4 and 11% of wildtype BubR1 levels. The *Bub1b*<sup>H/H</sup>, *Bub1b*<sup>H/+</sup>, *Bub1b*<sup>-/+</sup>, and *Bub1b*<sup>+/+</sup> MEFs were assessed for nocodazole-induced mitotic arrest, persistence of cdc2/cyclin B1 kinase activity, and presence of lagging chromosomes (also known as premature sister chromatid separation) as an indicator of chromosomal missegregation. Of these, only *Bub1b*<sup>H/H</sup> MEFs showed deficient nocodazole-induced arrest, decreased cdc2/cyclin B1 kinase activity, and increased lagging chromosomes. Interestingly, in contrast to an earlier study, the *Bub1b*<sup>-/+</sup>, and *Bub1b*<sup>+/+</sup> MEFs and animals appeared similar in every regard, and no increased aneuploidy or deficient mitotic checkpoint response was noted in the *Bub1b*<sup>-/+</sup> MEFs.

The hypomorphic mice showed further surprises. The *Bub1b*<sup>H/H</sup> mice generated were followed until 15-16 months of age. Six of the moribund or deceased *Bub1b*<sup>H/H</sup> mice were found to have solitary tumours, one of which was life-threatening. Even more striking was the shortened lifespan and the appearance of accelerated aging in mice starting at 2-3 months of age. The mice showed progressive development of cataracts, thinning of dermis and subcutaneous fat, cachexia, and lordokyphosis, all hallmarks of aging. None of these were observed in *Bub1b*<sup>H/+</sup>, *Bub1b*<sup>-/+</sup>, or *Bub1b*<sup>+/+</sup> mice. The physical appearance of the *Bub1b*<sup>H/H</sup> mice strikingly suggested early aging. But how was this related to a deficient mitotic checkpoint? Was the checkpoint deficiency somehow leading to increased cell death? Mice were therefore assessed for senescence and apoptosis. Beta-galactosidase activity is increased in senescent cells and so can be usefully employed as a visual assay when tissue sections are exposed to a substrate that turns blue to indicate activity of the enzyme. The kidney sections of five month old *Bub1b*<sup>H/H</sup> mice showed abundant beta-galactosidase activity, which was barely detectable in the tissues of wildtype and other BubR1-deficient backgrounds. MEFs from *Bub1b*<sup>H/H</sup> mice were also investigated for the response to hypoxia and were found to readily undergo apoptosis when oxygen concentration was lowered from the normal 20 to 3%. This suggested the lack of BubR1 resulted in heightened apoptosis under

conditions of oxidative stress. To further establish the link between lack of BubR1 and aging, BubR1 protein expression levels in the testis of wildtype mice were assessed via immunoblotting. Together these results suggested that deficient mitotic checkpoint control due to lack of BubR1 led to increased apoptosis and early senescence.

One additional aspect the BubR1 hypomorphic mice bears special mention. Karyotypic analyses of passage five MEFs from *Bub1b*<sup>H/H</sup> mice showed that 36% were aneuploid, almost four times the incidence in wildtype mice. Karyotypic analyses of adult splenocytes showed 33% were aneuploid by twelve months of age, with an increased incidence detectable even as early as two months. The degree of aneuploidy is far greater than the eventual incidence of tumour formation in these animals.

#### 4. DOES ANEUPLOIDY DIRECTLY PROMOTE CANCER?

The mouse models clearly showed that aneuploidy by itself often does not lead to tumour formation during an average lifespan. Similarly, the low frequency of mutations in mitotic checkpoint genes in human cancers suggests that they may not be the primary event that triggered chromosome instability. Consistent with the relative inefficiency of aneuploidy as a direct cause of cancer, in the report linking BubR1 mutations to mosaic variegated aneuploidy discussed earlier, malignancies were not identified in six of the eight families studied. The combined data therefore suggest that aneuploidy resulting from impairment of the mitotic checkpoint appears to be at best an inefficient mechanism in promoting tumorigenesis. Perhaps the events giving rise to the development of a cancer phenotype concurrently gave rise to aneuploidy. It has been proposed that defects in the mitotic checkpoint may confer a growth advantage to cancer cells, by enabling cells to tolerate chromosomal anomalies that normally would invoke a cell cycle arrest (see below).

If aneuploidy in many or most cancer cell lines does not arise from deficient mitotic checkpoint control, then where does it stem from? In recent years, it has become apparent that aneuploidy and carcinogenesis can arise from defects in DNA replication or recombination control. In contrast to the surprising lack of early transformation in cell lines deficient in the mitotic checkpoint proteins or early tumorigenesis in animals haplodeficient for these genes, a number of syndromes involving defects in DNA replication or recombination control have been identified in which chromosomal instability, aneuploidy, and increased tumorigenesis are prominent hallmarks. These include ataxia-telangiectasia, xeroderma pigmentosum, Nijmegen breakage syndromes, Bloom's syndrome, and Werner's syndrome, (Modesti and Kanaar, 2001; Thompson and Schild, 2002). Defects in mitotic checkpoint control have not been described for

these syndromes, nor do they seem required for the chromosomal instability characteristic of these syndromes. Rather, aneuploidy appears to stem from aberrant chromosomal duplication and deletions during homologous recombination occurring prior to the onset of mitosis. The net effect of such “unnatural acts” repeated over many cell cycles could be the deletion or duplication of large parts of or entire chromosomes, and potentially the deletion of genes encoding components of the mitotic checkpoint. Thus, the development of aneuploidy may antedate mitosis itself.

## 5. THE MITOTIC CHECKPOINT AS A TARGET FOR CANCER TREATMENT: WALKING A TIGHTROPE

Microtubule inhibitors are widely used in the clinic to treat a variety of cancers. Given our current understanding of the mitotic checkpoint, it would seem that this may be an important factor that dictates sensitivity of tumours to these drugs. Indeed, there appears to be some correlation between expression of mitotic checkpoint proteins and sensitivity to anti-microtubule agents (Masuda et al., 2003). Breast and ovarian cancer cell lines that showed little or no expression of one or more mitotic checkpoint proteins were sensitive to rapid killing by nocodazole and paclitaxel (Lee et al., 2004). In contrast, cells derived from cervical, colorectal, and renal cancers that showed stronger expression of these proteins and intact mitotic checkpoint control, were found to be relatively more resistant to killing by the same drugs. Importantly, abrogation of the mitotic checkpoint by RNA interference (RNAi) efficiently reversed drug resistance. Similarly, abrogation of mitotic checkpoint via the stable expression of RNAi targeting Mad2 and BubR1 led to massive chromosomal loss and cell death within six cell divisions (Kops et al., 2004). Antisense and ribozyme-mediated inhibition of Bub1 in normal human fibroblasts resulted in chromosome instability and massive nuclear fragmentation in many cells (Musio et al., 2003). Cells developed anchorage independence in soft agar and did not form tumours when injected into nude mice. Additional evidence supporting the idea that highly aneuploid cells are often non-viable came from the analysis of mSds3, an essential component of the mSin3/HDAC corepressor complex (David et al., 2003). mSds3 is essential in mice and MEF's lacking mSds3 exhibited defects in pericentric heterochromatin formation that interfered with centromere function. These cells were massively aneuploid and were largely inviable.

That disruption of the mitotic checkpoint leads to cell death may be an oversimplification as there is ample evidence supporting the idea that loss of the checkpoint promotes cell proliferation. The most striking example comes from the studies of the breast cancer susceptibility gene BRAC2. BRAC2 is an essential gene in mice and MEF's isolated from functionally

null BRCA2 mutant embryos exhibit poor growth in vitro as a result of elevated p53 and p21 that were induced by DNA damage (Lee et al., 1999). This growth defect was overcome by expressing either dominant negative p53 or Bub1 mutants. More interestingly, lymphomas isolated from the rare BRCA2 deficient mice that survived to adulthood, were found to be mutated in p53, Bub1 and BubR1. Thus, disruption of p53 and the mitotic checkpoint must cooperate with the BRCA2 mutation to promote cell transformation and uncontrolled proliferation. The intriguing relationship between BRCA2 and mitotic checkpoint control also highlights the notion that aneuploidy by itself does not promote cellular transformation efficiently. Thus, disruption of the mitotic checkpoint may be a secondary event that provides added growth advantage to cells that have undergone a transforming event.

How can we reconcile the difference as to whether cells proliferate or die when the mitotic checkpoint is disrupted? One reasonable explanation might be the degree to which the mitotic checkpoint is inhibited. If the checkpoint is completely eliminated, chromosomes have little to no time to align before cells exit mitosis. Consequently, cells undergo massive chromosome loss (or gain) that is incompatible with life. This would be consistent with the fact that mitotic checkpoint genes are essential in mice (and probably all mammals). On the other hand, heterozygous mutations, such as those identified in the BRCA2 mutant mice, or those reported in some human cancers, may retain sufficient checkpoint activity to allow cells to proceed through mitosis normally most of the time. The chromosome loss rate per generation may be sufficiently low that a large proportion of the population continues to proliferate. Along this line, it is also noteworthy that there is also selective pressure for mutations that cripple but do not obliterate the mitotic checkpoint. In other words, the mutations found in checkpoint genes of tumours may have been selected for so as to allow cells to proliferate in face of chromosomal defects.

## 6. CONCLUDING REMARKS

The recent efforts to understand the mechanism of action of the mitotic checkpoint mechanism can provide some insights into the mechanism of aneuploidy and its relationship to cancer. The current information indicates that mutations in mitotic checkpoint genes are rare in cancers. Despite this, many cancer cell lines still exhibit defects in the mitotic checkpoint (cannot arrest in response to microtubule inhibitors). This would suggest that additional genes are involved in the mitotic checkpoint. On the other hand, an important consideration is that the activity of the mitotic checkpoint is dosage dependent. There are examples where inactivation of the checkpoint was attributed to the reduced expression of one of the mitotic checkpoint genes. There is also experimental evidence that mutations in genes that are responsible for recruiting checkpoint proteins to the kinetochore could

effectively reduce their capacity to generate the “wait anaphase” signal. The mitotic checkpoint potential of a cell is therefore not merely dictated by the level of its checkpoint proteins but must include all the components of the system that include the APC/C, the amount of APC/C substrates, and the efficiency by which kinetochores establish productive interactions with the spindle.

The difference in the mitotic checkpoint status of cancer cells may be correlated with their sensitivity to drugs that interfere with spindle functions. The taxanes have shown modest or low efficacy in controlling sarcoma, colorectal, (squamous cell) cervical and renal cancers, (Edmonson et al., 1996; Hartmann and Bokemeyer, 1999; McGuire et al., 1996; Patel et al., 1996), cancers that appear to retain the mitotic checkpoint response when grown as cell lines in the laboratory. In contrast, the taxanes have been effective for and have become or will become standard chemotherapeutic treatment for patients afflicted with lung, breast, prostate, and ovarian cancers (Crown et al., 2004; Nowak et al., 2004; Patel et al., 1996; Petrylak and de Wit, 2002; Piccart et al., 2003; Picus and Schultz, 1999; Rigas, 2004; Shepherd, 2004). Consequently, effective clinical screens should be developed to profile the mitotic checkpoint status of tumours. This information would be of value in predicting outcome to treatment with current drugs such as the taxanes. Cells that have intact checkpoints may require longer regimens of drug infusion to ensure that the cancer cells do not simply rely on their checkpoint to overcome the drug treatment. Thus longer periods of drug exposure may improve tumour response. As increased exposure to drugs increases undesirable side effects, pharmacological inhibitors of the mitotic checkpoint should significantly enhance sensitivity of cancer cells to existing microtubule inhibitors. For example, inhibitors of the aurora kinases, seemed to selectively prevent cells treated with Taxol from arresting in mitosis (Ditchfield et al., 2003; Hauf et al., 2003). As Taxol treatment reduces kinetochore tension that is normally monitored by aurora B kinase, inhibitors of aurora B would be expected to sensitise cells to Taxol treatment. As inhibition of aurora B results in the loss of other kinetochore proteins that contribute towards the mitotic checkpoint, it remains to be seen if inhibition of those proteins might also sensitize cells to Taxol treatment. Regardless, it is clear that significant advances in cancer treatment will be achieved through continued efforts to elucidate the molecular and biochemical mechanisms that ensure accurate chromosome segregation.

## ACKNOWLEDGEMENTS

The authors would like to thank the respective lab members for advice and discussion in preparing this chapter. Research in TJY's lab is supported by the NIH (GM44762, CA099423, Core Grants CA75138, CA06927) U.S. Department of Defense. Research in GDK's lab is supported by U.S.

Department of Defense (ARCD-024-02F), the NIH (CA-R01CA107956), the University of Pennsylvania Cancer Center Foundation. Both labs are also supported by an appropriation from the Commonwealth of Pennsylvania.

## REFERENCES

- Andrews, P.D., E. Knatko, W.J. Moore, and J.R. Swedlow. 2003. Mitotic mechanics: the auroras come into view. *Curr Opin Cell Biol.* 15:672-83.
- Andrews, P.D., Y. Ovechkina, N. Morrice, M. Wagenbach, K. Duncan, L. Wordeman, and J.R. Swedlow. 2004. Aurora B regulates MCAK at the mitotic centromere. *Dev Cell.* 6:253-68.
- Babu, J.R., K.B. Jeganathan, D.J. Baker, X. Wu, N. Kang-Decker, and J.M. van Deursen. 2003. Rael is an essential mitotic checkpoint regulator that cooperates with Bub3 to prevent chromosome missegregation. *J Cell Biol.* 160:341-53.
- Baker, D.J., K.B. Jeganathan, J.D. Cameron, M. Thompson, S. Juneja, A. Kopecka, R. Kumar, R.B. Jenkins, P.C. de Groen, P. Roche, and J.M. van Deursen. 2004. BubR1 insufficiency causes early onset of aging-associated phenotypes and infertility in mice. *Nat Genet.* 36:744-9.
- Biggins, S., and C.E. Walczak. 2003. Captivating capture: how microtubules attach to kinetochores. *Curr Biol.* 13:R449-60.
- Cahill, D.P., L.T. da Costa, E.B. Carson-Walter, K.W. Kinzler, B. Vogelstein, and C. Lengauer. 1999. Characterization of MAD2B and other mitotic spindle checkpoint genes. *Genomics.* 58:181-7.
- Cahill, D.P., C. Lengauer, J. Yu, G.J. Riggins, J.K. Willson, S.D. Markowitz, K.W. Kinzler, and B. Vogelstein. 1998. Mutations of mitotic checkpoint genes in human cancers. *Nature.* 392:300-3.
- Chan, G.K., and T.J. Yen. 2003. The mitotic checkpoint: a signaling pathway that allows a single unattached kinetochore to inhibit mitotic exit. *Prog Cell Cycle Res.* 5:431-9.
- Chen, R.H., J.C. Waters, E.D. Salmon, and A.W. Murray. 1996. Association of spindle assembly checkpoint component XMD2 with unattached kinetochores. *Science.* 274:242-6.
- Cimini, D., B. Howell, P. Maddox, A. Khodjakov, F. Degrossi, and E.D. Salmon. 2001. Merotelic kinetochore orientation is a major mechanism of aneuploidy in mitotic mammalian tissue cells. *J Cell Biol.* 153:517-27.
- Clute, P., and J. Pines. 1999. Temporal and spatial control of cyclin B1 destruction in metaphase. *Nat Cell Biol.* 1:82-7.
- Crown, J., M. O'Leary, and W.S. Ooi. 2004. Docetaxel and paclitaxel in the treatment of breast cancer: a review of clinical experience. *Oncologist.* 9 Suppl 2:24-32.
- Dai, W., Q. Wang, T. Liu, M. Swamy, Y. Fang, S. Xie, R. Mahmood, Y.M. Yang, M. Xu, and C.V. Rao. 2004. Slippage of mitotic arrest and enhanced tumor development in mice with BubR1 haploinsufficiency. *Cancer Res.* 64:440-5.
- David, G., G.M. Turner, Y. Yao, A. Protopopov, and R.A. DePinho. 2003. mSin3-associated protein, mSds3, is essential for pericentric heterochromatin formation and chromosome segregation in mammalian cells. *Genes Dev.* 17:2396-405.
- DeLuca, J.G., B.J. Howell, J.C. Canman, J.M. Hickey, G. Fang, and E.D. Salmon. 2003. Nuf2 and Hec1 are required for retention of the checkpoint proteins Mad1 and Mad2 to kinetochores. *Curr Biol.* 13:2103-9.
- den Elzen, N., and J. Pines. 2001. Cyclin A is destroyed in prometaphase and can delay chromosome alignment and anaphase. *J Cell Biol.* 153:121-36.

- Ditchfield, C., V.L. Johnson, A. Tighe, R. Ellston, C. Haworth, T. Johnson, A. Mortlock, N. Keen, and S.S. Taylor. 2003. Aurora B couples chromosome alignment with anaphase by targeting BubR1, Mad2, and Cenp-E to kinetochores. *J Cell Biol.* 161:267-80.
- Dobles, M., V. Liberal, M.L. Scott, R. Benezra, and P.K. Sorger. 2000. Chromosome missegregation and apoptosis in mice lacking the mitotic checkpoint protein Mad2. *Cell.* 101:635-45.
- Edmonson, J.H., L.P. Ebbert, A.G. Nascimento, S.H. Jung, H. McGaw, and J.B. Gerstner. 1996. Phase II study of docetaxel in advanced soft tissue sarcomas. *Am J Clin Oncol.* 19:574-6.
- Fang, G., H. Yu, and M.W. Kirschner. 1998. The checkpoint protein MAD2 and the mitotic regulator CDC20 form a ternary complex with the anaphase-promoting complex to control anaphase initiation. *Genes Dev.* 12:1871-83.
- Fodde, R., J. Kuipers, C. Rosenberg, R. Smits, M. Kielman, C. Gaspar, J.H. van Es, C. Breukel, J. Wiegant, R.H. Giles, and H. Clevers. 2001. Mutations in the APC tumour suppressor gene cause chromosomal instability. *Nat Cell Biol.* 3:433-8.
- Geley, S., E. Kramer, C. Gieffers, J. Gannon, J.M. Peters, and T. Hunt. 2001. Anaphase-promoting complex/cyclosome-dependent proteolysis of human cyclin A starts at the beginning of mitosis and is not subject to the spindle assembly checkpoint. *J Cell Biol.* 153:137-48.
- Gemma, A., Y. Hosoya, M. Seike, K. Uematsu, F. Kurimoto, S. Hibino, A. Yoshimura, M. Shibuya, S. Kudoh, and M. Emi. 2001. Genomic structure of the human MAD2 gene and mutation analysis in human lung and breast cancers. *Lung Cancer.* 32:289-95.
- Gorbsky, G.J., R.H. Chen, and A.W. Murray. 1998. Microinjection of antibody to Mad2 protein into mammalian cells in mitosis induces premature anaphase. *J Cell Biol.* 141:1193-205.
- Hanks S, Coleman K, Reid S, Plaja A, Firth H, Fitzpatrick D, Kidd A, Mehes K, Nash R, Robin N, Shannon N, Tolmie J, Swansbury J, Irrthum A, Douglas J, Rahman N. 2004. Constitutional aneuploidy and cancer predisposition caused by biallelic mutations in BUB1B. *Nat Genet.* 36 (11):1159-61.
- Hartmann, J.T., and C. Bokemeyer. 1999. Chemotherapy for renal cell carcinoma. *Anticancer Res.* 19:1541-3.
- Hauf, S., R.W. Cole, S. LaTerra, C. Zimmer, G. Schnapp, R. Walter, A. Heckel, J. van Meel, C.L. Rieder, and J.M. Peters. 2003. The small molecule Hesperadin reveals a role for Aurora B in correcting kinetochore-microtubule attachment and in maintaining the spindle assembly checkpoint. *J Cell Biol.* 161:281-94.
- Hernando, E., I. Orlow, V. Liberal, G. Nohales, R. Benezra, and C. Cordon-Cardo. 2001. Molecular analyses of the mitotic checkpoint components hMAD2, hBUB1 and hBUB3 in human cancer. *Int J Cancer.* 95:223-7.
- Hoffman, D.B., C.G. Pearson, T.J. Yen, B.J. Howell, and E.D. Salmon. 2001. Microtubule-dependent changes in assembly of microtubule motor proteins and mitotic spindle checkpoint proteins at PtK1 kinetochores. *Mol Biol Cell.* 12:1995-2009.
- Howell, B.J., D.B. Hoffman, G. Fang, A.W. Murray, and E.D. Salmon. 2000. Visualization of Mad2 dynamics at kinetochores, along spindle fibers, and at spindle poles in living cells. *J Cell Biol.* 150:1233-50.
- Imai, Y., Y. Shiratori, N. Kato, T. Inoue, and M. Omata. 1999. Mutational inactivation of mitotic checkpoint genes, hMAD2 and hBUB1, is rare in sporadic digestive tract cancers. *Jpn J Cancer Res.* 90:837-40.
- Johnson, V.L., M.I. Scott, S.V. Holt, D. Hussein, and S.S. Taylor. 2004. Bub1 is required for kinetochore localization of BubR1, Cenp-E, Cenp-F and Mad2, and chromosome congression. *J Cell Sci.* 117:1577-89.
- Kaplan, K.B., A.A. Burds, J.R. Swedlow, S.S. Bekir, P.K. Sorger, and I.S. Nathke. 2001. A role for the Adenomatous Polyposis Coli protein in chromosome segregation. *Nat Cell Biol.* 3:429-32.



## 4.3. Mitotic Checkpoint, Aneuploidy and Cancer

497

- King, R.W., J.M. Peters, S. Tugendreich, M. Rolfe, P. Hieter, and M.W. Kirschner. 1995. A 20S complex containing CDC27 and CDC16 catalyzes the mitosis-specific conjugation of ubiquitin to cyclin B. *Cell*. 81:279-88.
- Kops, G.J., D.R. Foltz, and D.W. Cleveland. 2004. Lethality to human cancer cells through massive chromosome loss by inhibition of the mitotic checkpoint. *Proc Natl Acad Sci U S A*. 101:8699-704.
- Lan, W., X. Zhang, S.L. Kline-Smith, S.E. Rosasco, G.A. Barrett-Wilt, J. Shabanowitz, D.F. Hunt, C.E. Walczak, and P.T. Stukenberg. 2004. Aurora B phosphorylates centromeric MCAK and regulates its localization and microtubule depolymerization activity. *Curr Biol*. 14:273-86.
- Lee, E.A., M.K. Keutmann, M.L. Dowling, E. Harris, G. Chan, and G.D. Kao. 2004. Inactivation of the mitotic checkpoint as a determinant of the efficacy of microtubule-targeted drugs in killing human cancer cells. *Mol Cancer Ther*. 3:661-9.
- Lee, H., A.H. Trainer, L.S. Friedman, F.C. Thistlethwaite, M.J. Evans, B.A. Ponder, and A.R. Venkitaraman. 1999. Mitotic checkpoint inactivation fosters transformation in cells lacking the breast cancer susceptibility gene, Brca2. *Mol Cell*. 4:1-10.
- Lengauer, C., K.W. Kinzler, and B. Vogelstein. 1998. Genetic instabilities in human cancers. *Nature*. 396:643-9.
- Li, X., and R.B. Nicklas. 1995. Mitotic forces control a cell-cycle checkpoint. *Nature*. 373:630-2.
- Li, Y., and R. Benezra. 1996. Identification of a human mitotic checkpoint gene: hSMAD2. *Science*. 274:246-8.
- Liu, S.T., J.C. Hittle, S.A. Jablonski, M.S. Campbell, K. Yoda, and T.J. Yen. 2003. Human CENP-I specifies localization of CENP-F, MAD1 and MAD2 to kinetochores and is essential for mitosis. *Nat Cell Biol*. 5:341-5.
- Loeb, L.A. 1991. Mutator phenotype may be required for multistage carcinogenesis. *Cancer Res*. 51:3075-9.
- Luo, X., G. Fang, M. Coldiron, Y. Lin, H. Yu, M.W. Kirschner, and G. Wagner. 2000. Structure of the Mad2 spindle assembly checkpoint protein and its interaction with Cdc20. *Nat Struct Biol*. 7:224-9.
- Luo, X., Z. Tang, G. Xia, K. Wassmann, T. Matsumoto, J. Rizo, and H. Yu. 2004. The Mad2 spindle checkpoint protein has two distinct natively folded states. *Nat Struct Mol Biol*. 11:338-45.
- Martin-Lluesma, S., V.M. Stucke, and E.A. Nigg. 2002. Role of hcc1 in spindle checkpoint signaling and kinetochore recruitment of mad1/mad2. *Science*. 297:2267-70.
- Masuda, A., K. Maeno, T. Nakagawa, H. Saito, and T. Takahashi. 2003. Association between mitotic spindle checkpoint impairment and susceptibility to the induction of apoptosis by anti-microtubule agents in human lung cancers. *Am J Pathol*. 163:1109-16.
- McEwen, B.F., G.K. Chan, B. Zubrowski, M.S. Savoian, M.T. Sauer, and T.J. Yen. 2001. CENP-E is essential for reliable bioriented spindle attachment, but chromosome alignment can be achieved via redundant mechanisms in mammalian cells. *Mol Biol Cell*. 12:2776-89.
- McGuire, W.P., J.A. Blessing, D. Moore, S.S. Lentz, and G. Photopulos. 1996. Paclitaxel has moderate activity in squamous cervix cancer. A Gynecologic Oncology Group study. *J Clin Oncol*. 14:792-5.
- Meraldi, P., V.M. Draviam, and P.K. Sorger. 2004. Timing and checkpoints in the regulation of mitotic progression. *Dev Cell*. 7:45-60.
- Modesti, M., and R. Kanaar. 2001. Homologous recombination: from model organisms to human disease. *Genome Biol*. 2:REVIEWS1014.
- Musio, A., C. Montagna, D. Zamboni, E. Indino, O. Barbieri, L. Citti, A. Villa, T. Ried, and P. Vezzone. 2003. Inhibition of BUB1 Results in Genomic Instability and Anchorage-independent Growth of Normal Human Fibroblasts. *Cancer Res*. 63:2855-63.
- Nicklas, R.B. 1997. How cells get the right chromosomes. *Science*. 275:632-7.

- Nicklas, R.B., and S.C. Ward. 1994. Elements of error correction in mitosis: microtubule capture, release, and tension. *J Cell Biol.* 126:1241-53.
- Nowak, A.K., N.R. Wilcken, M.R. Stockler, A. Hamilton, and D. Gherzi. 2004. Systematic review of taxane-containing versus non-taxane-containing regimens for adjuvant and neoadjuvant treatment of early breast cancer. *Lancet Oncol.* 5:372-80.
- Ohshima, K., S. Haraoka, S. Yoshioka, M. Hamasaki, T. Fujiki, J. Suzumiya, C. Kawasaki, M. Kanda, and M. Kikuchi. 2000. Mutation analysis of mitotic checkpoint genes (hBUB1 and hBUBR1) and microsatellite instability in adult T-cell leukemia/lymphoma. *Cancer Lett.* 158:141-50.
- Orr-Weaver, T.L., and R.A. Weinberg. 1998. A checkpoint on the road to cancer. *Nature.* 392:223-4.
- Pan, J., and R.H. Chen. 2004. Spindle checkpoint regulates Cdc20p stability in *Saccharomyces cerevisiae*. *Genes Dev.* 18:1439-51.
- Patel, S.R., N.E. Papadopoulos, C. Plager, K.A. Linke, S.H. Moseley, C.H. Spiridonidis, and R. Benjamin. 1996. Phase II study of paclitaxel in patients with previously treated osteosarcoma and its variants. *Cancer.* 78:741-4.
- Percy, M.J., K.A. Myrie, C.K. Neeley, J.N. Azim, S.P. Ethier, and E.M. Petty. 2000. Expression and mutational analyses of the human MAD2L1 gene in breast cancer cells. *Genes Chromosomes Cancer.* 29:356-62.
- Petrylak, D.P., and R. de Wit. 2002. Editorial: the coming revolution in the treatment of prostate cancer patients. *Semin Urol Oncol.* 20:1-3.
- Piccart, M.J., K. Bertelsen, G. Stuart, J. Cassidy, C. Mangioni, E. Simonsen, K. James, S. Kaye, I. Vergote, R. Blom, R. Grimshaw, R. Atkinson, K. Swenerton, C. Trope, M. Nardi, J. Kaern, S. Tumolo, P. Timmers, J.A. Roy, F. Lhoas, B. Lidvall, M. Bacon, A. Birt, J. Andersen, B. Zee, J. Paul, S. Pecorelli, B. Baron, and W. McGuire. 2003. Long-term follow-up confirms a survival advantage of the paclitaxel-cisplatin regimen over the cyclophosphamide-cisplatin combination in advanced ovarian cancer. *Int J Gynecol Cancer.* 13 Suppl 2:144-8.
- Picus, J., and M. Schultz. 1999. Docetaxel (Taxotere) as monotherapy in the treatment of hormone-refractory prostate cancer: preliminary results. *Semin Oncol.* 26:14-8.
- Pihan, G.A., and S.J. Doxsey. 1999. The mitotic machinery as a source of genetic instability in cancer. *Semin Cancer Biol.* 9:289-302.
- Putkey, F.R., T. Cramer, M.K. Morphey, A.D. Silk, R.S. Johnson, J.R. McIntosh, and D.W. Cleveland. 2002. Unstable kinetochore-microtubule capture and chromosomal instability following deletion of CENP-E. *Dev Cell.* 3:351-65.
- Reis, R.M., M. Nakamura, J. Masuoka, T. Watanabe, S. Colella, Y. Yonekawa, P. Kleihues, and H. Ohgaki. 2001. Mutation analysis of hBUB1, hBUBR1 and hBUB3 genes in glioblastomas. *Acta Neuropathol (Berl).* 101:297-304.
- Rieder, C.L., and E.D. Salmon. 1994. Motile kinetochores and polar ejection forces dictate chromosome position on the vertebrate mitotic spindle. *J Cell Biol.* 124:223-33.
- Rigas, J.R. 2004. Taxane-platinum combinations in advanced non-small cell lung cancer: a review. *Oncologist.* 9 Suppl 2:16-23.
- Ru, H.Y., R.L. Chen, W.C. Lu, and J.H. Chen. 2002. hBUB1 defects in leukemia and lymphoma cells. *Oncogene.* 21:4673-9.
- Sato, M., Y. Sekido, Y. Horio, M. Takahashi, H. Saito, J.D. Minna, K. Shimokata, and Y. Hasegawa. 2000. Infrequent mutation of the hBUB1 and hBUBR1 genes in human lung cancer. *Jpn J Cancer Res.* 91:504-9.
- Schaar, B.T., G.K.T. Chan, P. Maddox, E.D. Salmon, and T.J. Yen. 1997. CENP-E function at kinetochores is essential for chromosome alignment. *J. Cell Biol.* 139:1373-1382.
- Shannon, K.B., J.C. Canman, and E.D. Salmon. 2002. Mad2 and BubR1 function in a single checkpoint pathway that responds to a loss of tension. *Mol Biol Cell.* 13:3706-19.
- Shepherd, F.A. 2004. Current paradigms in first-line treatment of non-small-cell lung cancer. *Oncology (Huntingt).* 18:13-20.

## 4.3. Mitotic Checkpoint, Aneuploidy and Cancer

499

- Shichiri, M., K. Yoshinaga, H. Hisatomi, K. Sugihara, and Y. Hirata. 2002. Genetic and epigenetic inactivation of mitotic checkpoint genes hBUB1 and hBUBR1 and their relationship to survival. *Cancer Res.* 62:13-7.
- Skibbens, R.V., and P. Hieter. 1998. Kinetochore and the checkpoint mechanism that monitors for defects in the chromosome segregation machinery. *Annu Rev Genet.* 32:307-37.
- Skoufias, D.A., P.R. Andreassen, F.B. Lacroix, L. Wilson, and R.L. Margolis. 2001. Mammalian mad2 and bub1/bubR1 recognize distinct spindle-attachment and kinetochore-tension checkpoints. *Proc Natl Acad Sci U S A.* 98:4492-7.
- Sudakin, V., G.K. Chan, and T.J. Yen. 2001. Checkpoint inhibition of the APC/C in HeLa cells is mediated by a complex of BUBR1, BUB3, CDC20, and MAD2. *J Cell Biol.* 154:925-36.
- Sudakin, V., D. Ganoh, A. Dahan, H. Heller, J. Hershko, F.C. Luca, J.V. Ruderman, and A. Hershko. 1995. The cyclosome, a large complex containing cyclin-selective ubiquitin ligase activity, targets cyclins for destruction at the end of mitosis. *Mol Biol Cell.* 6:185-97.
- Takahashi, T., N. Haruki, S. Nomoto, A. Masuda, S. Saji, and H. Osada. 1999. Identification of frequent impairment of the mitotic checkpoint and molecular analysis of the mitotic checkpoint genes, hSMAD2 and p55CDC, in human lung cancers. *Oncogene.* 18:4295-300.
- Tanaka, T.U., N. Rachidi, C. Janke, G. Pereira, M. Galova, E. Schiebel, M.J. Stark, and K. Nasmyth. 2002. Evidence that the Ipl1-Sli15 (Aurora kinase-INCENP) complex promotes chromosome bi-orientation by altering kinetochore-spindle pole connections. *Cell.* 108:317-29.
- Thompson, L.H., and D. Schild. 2002. Recombinational DNA repair and human disease. *Mutat Res.* 509:49-78.
- Tighe, A., V.L. Johnson, M. Albertella, and S.S. Taylor. 2001. Aneuploid colon cancer cells have a robust spindle checkpoint. *EMBO Rep.* 2:609-14.
- Tsukasaki, K., C.W. Miller, E. Greenspun, S. Eshaghian, H. Kawabata, T. Fujimoto, M. Tomonaga, C. Sawyers, J.W. Said, and H.P. Koeffler. 2001. Mutations in the mitotic checkpoint gene, MAD1L1, in human cancers. *Oncogene.* 20:3301-5.
- Wang, X., J.R. Babu, J.M. Harden, S.A. Jablonski, M.H. Gazi, W.L. Lingle, P.C. de Groen, T.J. Yen, and J.M. van Deursen. 2001. The mitotic checkpoint protein hBUB3 and the mRNA export factor hRAE1 interact with GLE2p-binding sequence (GLEBS)-containing proteins. *J Biol Chem.* 276:26559-67.
- Wang, X., D.Y. Jin, R.W. Ng, H. Feng, Y.C. Wong, A.L. Cheung, and S.W. Tsao. 2002. Significance of MAD2 expression to mitotic checkpoint control in ovarian cancer cells. *Cancer Res.* 62:1662-8.
- Wang, X., D.Y. Jin, Y.C. Wong, A.L. Cheung, A.C. Chun, A.K. Lo, Y. Liu, and S.W. Tsao. 2000. Correlation of defective mitotic checkpoint with aberrantly reduced expression of MAD2 protein in nasopharyngeal carcinoma cells. *Carcinogenesis.* 21:2293-7.
- Waters, J.C., R.H. Chen, A.W. Murray, and E.D. Salmon. 1998. Localization of Mad2 to kinetochores depends on microtubule attachment, not tension. *J Cell Biol.* 141:1181-91.
- Weaver, B.A., Z.Q. Bonday, F.R. Putkey, G.J. Kops, A.D. Silk, and D.W. Cleveland. 2003. Centromere-associated protein-E is essential for the mammalian mitotic checkpoint to prevent aneuploidy due to single chromosome loss. *J Cell Biol.* 162:551-63.
- Yao, X., A. Abrieu, Y. Zheng, K.F. Sullivan, and D.W. Cleveland. 2000. CENP-E forms a link between attachment of spindle microtubules to kinetochores and the mitotic checkpoint. *Nat Cell Biol.* 2:484-91.